INDC INTERNATIONAL NUCLEAR DATA COMMITTEE

RECOMMENDED ATOMIC DATA FOR HYDROGEN AND HELIUM PLASMAS

V.A. Abramov, L.A. Vainshtein, G.I. Krotova and A.Yu. Pigarov

USSR State Committee on the Utilization of Atomic Energy
Central Scientific Research Institute of Information
and Technoeconomic Studies on Atomic Science and Technology

July 1988

IAEA NUCLEAR DATA SECTION, WAGRAMERSTRASSE 5, A-1400 VIENNA
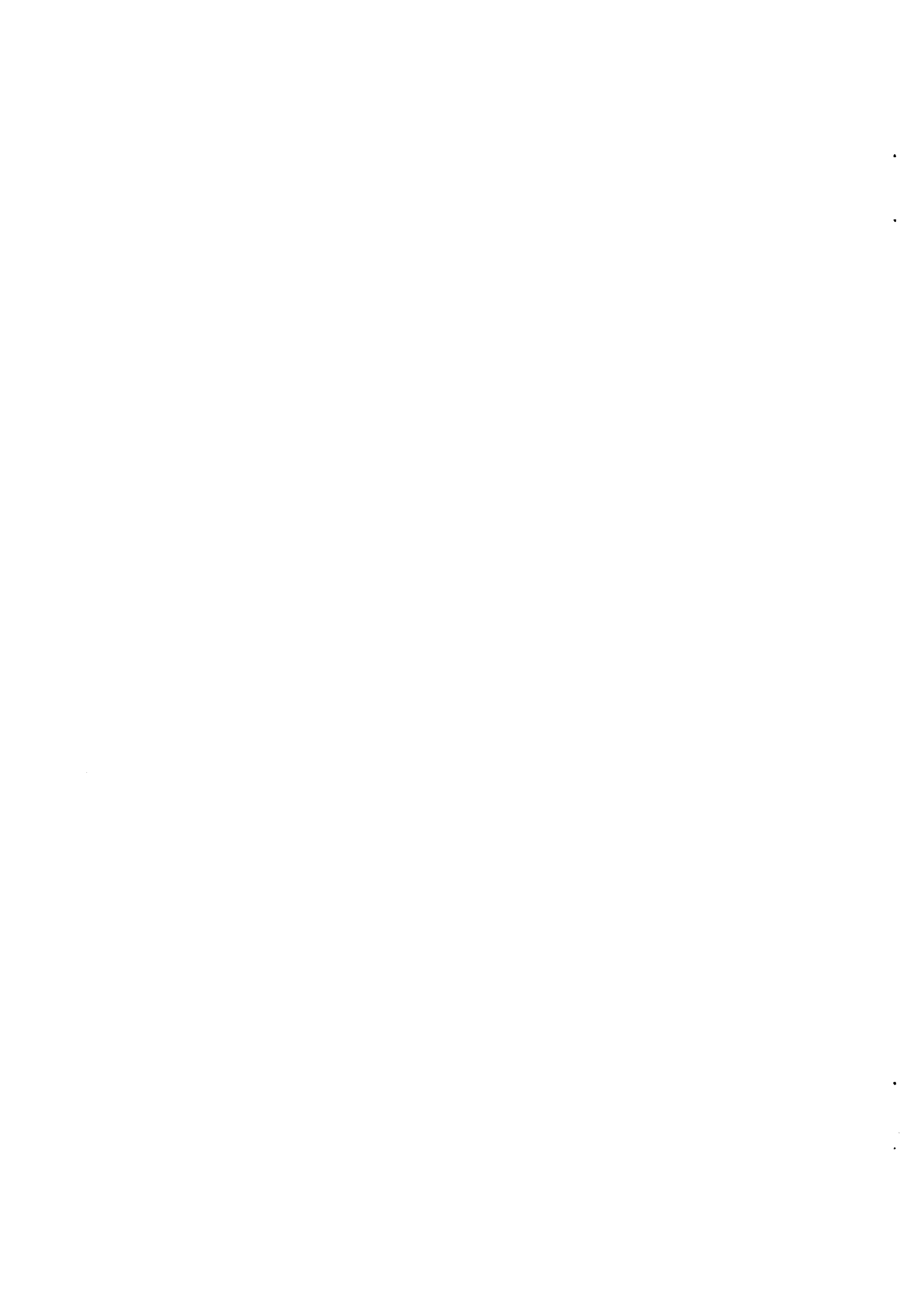
RECOMMENDED ATOMIC DATA FOR HYDROGEN AND HELIUM PLASMAS

V.A. Abramov, L.A. Vainshtein, G.I. Krotova and A.Yu. Pigarov

USSR State Committee on the Utilization of Atomic Energy
Central Scientific Research Institute of Information
and Technoeconomic Studies on Atomic Science and Technology

July 1988

I.   INTRODUCTION

In connection with the detailed development work in progress in a number of countries on designs of the tokamak reactor (OTR, INTOR, FER, NET) a good deal of attention is being devoted to resolving the problem of impurity flux control and removal of the helium produced from the burning of the D-T plasma. Evaluations show that the impurity content in the plasma should be such that Z_{eff} = 1.5. For this purpose, it is necessary to use various methods to prevent impurities from penetrating into the central part of the plasma column. Currently under consideration are either various types of divertors (poloidal and ergodic) or pump limiters. In any case, to shield the plasma from impurity fluxes one has to generate a sufficiently cold and dense boundary plasma layer. At present, for a number of reasons, the operation of the divertor (single-null or double-null) in a regime with a dense and relatively cold plasma (n_e = 10^{14} to 10^{16} cm^{-3}, T_e = 5 to 100 eV) is considered the most attractive. The divertor is also necessary for pumping helium. Evaluations show that about 10^{20} particles per second have to be pumped in order to maintain the relative helium content at a level not exceeding 5%. To determine the actual velocity of the pumping devices, we have to know as accurately as possible the concentration of neutral helium near the pumping nozzles. This value is determined by the dynamics of helium ions reaching the divertor and their interaction with the basic plasma ions (deuterium and tritium), electrons and impurity ions. Thus, to solve these two problems (determination of the shielding and pumping properties of the divertor), we should know how to determine the characteristics of the divertor plasma with a sufficiently high accuracy. It should be noted that for the above-mentioned plasma parameters, in determining the ionization state of the deuterium-tritium and helium plasmas in order to calculate the radiation losses in such a plasma, we need to consider the complete collisional-radiative model for determination of the level population of the hydrogen atoms (henceforth we shall everywhere neglect the isotopic effects and the

word "hydrogen" will refer to both deuterium and tritium) and of the helium atoms and ions, and that we cannot confine ourselves to considering the limiting cases (local thermodynamic equilibrium or coronal equilibrium). It is obvious that calculations by the collisional-radiative model require reliable data on the probabilities of various radiative transitions and on the collision cross- sections of electrons with hydrogen atoms and helium atoms (ions) for different inelastic processes. One must also note that the same data are also needed to solve a number of problems arising in low-temperature plasma physics and a number of diagnostic problems in both laboratory and astrophysical plasmas.

The analysis of data for electron collision cross-sections with helium atoms, which were collected earlier during the solution of some astrophysical problems, shows that the available information is very meagre and fragmentary. Moreover, the cross-section values for the same processes at identical energies given in different sources differ considerably and sometimes by an order of magnitude so that the data should be evaluated with sufficient care.

The situation is somewhat better with the data for the hydrogen atom, in which case for an extensive range of processes the electron collision cross-sections have been calculated in a large region of energies in using different approximations. Data on radiative transition probabilities can be obtained with any degree of accuracy, and the problem reduces essentially to representing the probability of radiative processes in a form sufficiently convenient for carrying out extensive numerical calculations.

The purpose of the present work is to analyse as much as possible the whole of the existing data on the helium atom, to calculate the required cross-sections (and reaction rates) in a number of cases and to represent the recommended cross-section (or reaction rate) values in a form convenient for practical use in the numerical modelling of the behaviour of the helium plasma in the region of relatively low electron temperatures (T_e = 3 to 100 eV).

4

In the case of hydrogen, we shall only give the results of comparison of the cross-section calculations for a number of processes contained in different studies and present the necessary data for the probabilities of radiative processes. We should point out that for helium we shall mainly analyse data obtained after 1978 since those published before 1978 are analysed in Ref. [1]. We must stress, in particular, that in the temperature region of interest to us the experimental data are very scanty.

II. KINETIC MODEL

In the collisional-radiative model developed in Ref. [2] and used later by a number of authors (see discussion in Ref. [3]) the change in the level population $N(n)$ of the hydrogen atom with the principal quantum number n is described by the coupled equations of the form:

$$\frac{dN(n)}{dt} = -N(n)[n_e K_{nc} + n_e \sum_{m \neq n} K_{nm} + \sum_{q < n} A(n,q)] + n_e \sum_{q \neq n} N(q)K_{qn} +$$

$$+ \sum_{q > n} N(q)A(q,n) + N(H^+)n_e^2 \alpha_{(n)}^{(3)} + N(H^+) \, n_e \alpha_{(n)}^{(2)}, \tag{1}$$

where K_{nc} is the ionization rate of state n, K_{qn} is the rate of the collisional transition $q \rightarrow n$, $A(q,n)$ is the probability of radiative transition $q \rightarrow n$, $N(H^+)$ is the proton density, $\alpha_{(n)}^{(3)}$ is the coefficient of three-body recombination into level n, and $\alpha_{(n)}^{(2)}$ is the coefficient of radiative recombination into level n. In the quasi-stationary approximation, which can be applied satisfactorily under the conditions considered (for more details see, for example Ref. [3]) all $\dot{N}(n) = 0$ except the level with n = 1 (ground state). Then, as is well known, the rate of change in the population of the first level is described by the equation:

$$\frac{dN(1)}{dt} = -S_{eff} \, n_e N(1) + \alpha_{eff} \, n_e N(H^+), \tag{2}$$

where S_{eff} is the effective ionization rate, which depends on the temperature T_e and electron density n_e (it is determined in a complex manner by the collisional and radiative transition probabilities) and α_{eff}

is the effective recombination coefficient, which depends also on T_e and n_e. Thus, by solving system (1) (using the condition $\dot{N}(n) = 0$ for $n \neq 1$) we can determine S_{eff}, α_{eff} and the populations of all excited states, i.e. all the charcteristics needed to calculate, for example, the radiation losses. In order to solve this sytem, we have obviously to know the values of K_{nc}, K_{nq}, $A(q,n)$, $\alpha_{(n)}^{(3)}$ and $\alpha_{(n)}^{(2)}$. The rates of the direct and inverse processes are connected with each other by the Klein-Rosseland relations so that we only need information on the rates of the corresponding direct processes (we assume that the electron distribution function is Maxwellian). The cross-sections for the direct and inverse processes are connected with each other by relations resulting from the detailed balance principle.

To calculate the level populations of the helium atom, we can use virtually the same system of equations (1). The difference from the hydrogen case is that the dielectronic recombination rate has to be added to coefficient $\alpha_{(n)}^{(2)}$ and that the numbering of levels for the helium atom does not coincide with the principal quantum number of the level. This is due to the fact that, in the case of helium, there is no accidental Coulomb degeneracy (i.e. the energy depends on n and on L, the orbital quantum number). However, the hydrogen approximation is applicable to the states of the helium atom with sufficiently large n since levels with the same n but different L have practically coinciding values of energy. The analysis of the energy spectrum structure (for details, see below) shows that for $n \geq 5$ the hydrogen-like approximation is valid. Therefore, in the case of a helium plasma, the data on the cross-sections of different collisional transitions for levels with n = 1 to 4 are of interest.

III. DATA BASE

1. STRUCTURE OF THE SPECTRA

For the sake of a complete description and convenience of use, we briefly review the systematics of the energy levels of the hydrogen and helium atoms.

The value of the level energy of the hydrogen atom with a principal quantum number n is determined, as is well known, by the expression:

$$E_n = - \frac{13,6}{n^2} \ [e\,V].$$ (3)

Under the conditions considered by us it can be assumed that the population of the sub-level $n\ell$ is determined by the statistical weight of this sub-level, i.e. by:

$$N(n\ell) = \frac{2\ell + 1}{n^2} \bar{N}(n).$$ (4)

For the hydrogen atom the probability of radiative transition between levels with principal quantum numbers n, n' (n is the upper state) can be determined from the relation:

$$A(n, n') = 8,014 \cdot 10^9 \ (\frac{1}{(n')^2} - \frac{1}{n^2})^2 \ f_{n'n} \frac{g_{n'}}{g_n} \ [s^{-1}],$$ (5)

where $f_{n'n}$ is the oscillator strength during absorption and g_n is the statistical weight of the level with principal quantum number n. The values of $f_{n'n}$ for a number of transitions can be found, for example, in Refs [4, 5]. In Ref. [6] the following approximation is suggested for $f_{n'n}$:

$$f_{n'n} = 2 \ \frac{n'}{(nx)^3} \varphi(n', x),$$ (6)

where

$$x = \frac{1}{(1/n'^2 - 1/n^2)} = \frac{(nn')^2}{(n^2 - n'^2)},$$

$$\varphi(n', x) = \varphi_0(n') + \varphi_1(n')/x + \varphi_2(n')/x^2,$$ (7)

$$\varphi_0(n') = \begin{cases} 1,133, & n' = 1, \\ 1,0785, & n' = 2, \\ 0,9835 + 0,2328/n' - 0,1296/(n')^2, & n' > 3, \end{cases}$$ (8)

7

$$\varphi_1(n') = \begin{cases} -0.4059, & n' = 1, \\ -0.2319, & n' = 2, \\ -(0.6282 - 0.5598/n' + 0.5299/(n')^2)/n', & n' > 3, \end{cases} \qquad (9)$$

$$\varphi_2(n') = \begin{cases} 0.07014, & n' = 1, \\ 0.02947, & n' = 2, \\ (0.3887 - 1.181/n' + 1.47/(n')^2)/n', & n' > 3. \end{cases} \qquad (10)$$

Unlike the hydrogen atom, the helium atom has two term systems – singlet (corresponding to the case S = 0, S being the total spin of the system of two electrons) and triplet (corresponding to the case S = 1). Moreover, in contrast to the hydrogen atom, the energies of levels with identical principal quantum number n but with different L are different. A partial term diagram of the helium atom is given in Fig. 1. It can be seen that the dependence of the term energy on L is substantial only for states with n < 5. Therefore, levels with n ≥ 5 can be regarded virtually as hydrogen-like. For this reason, in analysing the data on the cross-sections for transitions between different levels of the helium atom we shall henceforth confine ourselves to considering the transitions between levels with n = 1 to 4 for both the singlet and the triplet term system. It is convenient to analyse the helium data separately for the allowed transitions (Δℓ = ±1), forbidden transitions (Δℓ ≠ ±1, ΔS = 0) and intercombination transitions (ΔS ≠ 0). We first consider in greater detail the data for the helium atom and then compare the results of some calculations for the hydrogen atom.

2.   ANALYSIS OF COLLISION CROSS-SECTION DATA FOR THE HELIUM ATOM

2.1.   Allowed transitions

In this work we consider only the single-electron excited states, i.e. states of type 1snℓ, so that obviously L = ℓ (L now is the total orbital moment of the atom). In the LS-coupling scheme valid for the helium atom, dipole transitions are allowed in accordance with the following selection rules: ΔS = 0, ΔL = 0, ±1; L + L' ≥ 1 (L, L' are the orbital moments of states between which the transition occurs). Table 1 gives the values of transition energy, eV, oscillator strength during absorption and
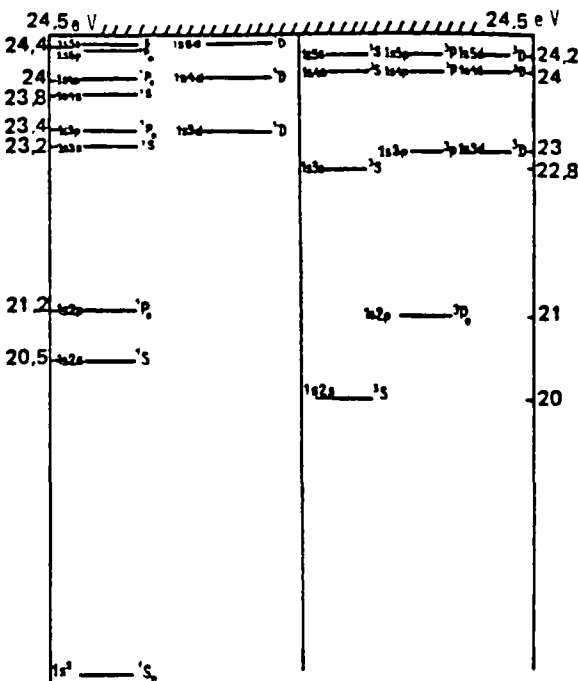
Fig. 1. Partial term diagram of the helium atom

Table 1

Transition	ΔE, eV	f_{abs} [5]	$A, 10^8\ s^{-1}$ [5]	f_{abs} ("Атом")
$2^1P - 1^1S_0$	20,5	0,276	17,99	0,310
$3^1P - 1^1S_0$	22,3	0,073	5,66	0,09
$4^1P - 1^1S_0$	22,98	0,03	2,46	0,034
$2^1P - 2^1S$	0,6	0,37	0,02	0,34
$3^1P - 2^1S$	2,4	0,15	0,13	0,16
$4^1P - 2^1S$	3,07	0,05	0,07	0,05
$3^1S - 2^1P$	1,6	0,04	0,19	0,04
$4^1S - 2^1P$	2,4	0,008	0,06	0,008
$3^1D - 2^1P$	1,8	0,711	0,64	0,69
$4^1D - 2^1P$	2,4	0,12	0,2	0,12
$4^1D - 3^1P$	0,63	0,647	0,07	0,615
$4^1S - 3^1P$	0,57	0,103	0,046	0,094
$2^3P - 2^3S$	1,2	0,54	0,1	0,54
$3^3P - 2^3S$	3,07	0,06	0,1	0,063
$4^3P - 2^3S$	3,75	0,02	0,05	0,025
$3^3S - 2^3P$	1,7	0,07	0,28	0,06
$3^3D - 2^3P$	2,07	0,6	0,7	0,67
$4^3D - 2^3P$	2,72	0,125	0,25	0,122
$4^3S - 3^3P$	0,57	0,145	0,06	0,145
$4^3P - 3^3S$	0,98	0,04	0,006	0,05
$4^3D - 3^3P$	0,7	0,48	0,067	0,48
$4^3S - 2^3P$	2,55	0,01	0,1	0,0098

radiative transition probability A, s^{-1}, in the group of levels with n = 1

to 4. The table contains the values of f taken from Ref. [5] and those

calculated by the "Atom" program described in detail in Ref. [7].

The data on the electron-impact excitation cross-sections for allowed transitions are given in Refs [8-21]. References [8-10, 21] contain experimental data and the remaining references give the results of calculation using different approximations. The studies referred to were carried out mainly by the usual methods of cross-section calculation. Thus, the R-matrix method is used in Refs [12, 19]; in Ref. [12], account is taken of the pseudo-states, which, in the opinion of its authors, lead to better values of polarizability than those in Ref. [11]. In Refs [13, 14] the method of distorted waves is used in the 30-200 eV region. In Ref. [14] it is shown that the existing differences between calculation results and experimental data can be reduced substantially if the contribution of the pseudostates is taken into account. Moreover, in Ref. [14] the calculation uses five different approximations for the wave functions (with and without allowance for exchange). It should be pointed out, however, that different methods are used for calculations of some, to a certain extent arbitrarily chosen, transitions in a very limited energy (temperature) region. Thus, in Ref. [20] data are given for 10 transitions in the region of T_e = 0.08 to 4.3 eV, whereas information is needed for hundreds of transitions in the T_e = 3-100 eV region. It is therefore necessary to calculate the cross-sections systematically. In the present study the electron-impact excitation cross-sections were calculated in the Born approximation with allowance for exchange and with normalization of the cross-sections by the K-matrix method. The normalization was performed to one eigenchannel [22]. Exchange was taken into account in most cases by the method of orthogonalized functions (for details, see Ref. [7]). It should be noted that in the case of transitions from the ground state of the helium atom the substractive procedure of orthogonalization becomes inefficient since each term is greater than the difference by an order of magnitude. In this case, a more stable method, suggested in Ref. [23], was used (see also Ref. [7]). Normalization with the help of the K-matrix cannot be used for the Ochkur method; however, for

10

transitions from the ground state the effect of normalization is small. The cross-sections were calculated numerically by the "Atom" program developed at the Physics Institute of the USSR Academy of Sciences (FIAN) (for a detailed description of this program, see Ref. [7]). After the numerical calculation, the cross-sections σ and excitation rates $<v\sigma>$ were approximated (using the method of least squares) by analytical functions with two parameters: C and φ (for σ) and A and χ (for $<v\sigma>$)*.

In the cross-section calculation we used the single-electron semi-empirical atomic functions, which are solutions of the Schrödinger single-electron equation with experimental energy level values and a scale factor in the potential. The same functions were utilized to calculate the oscillator strengths for absorption, which are given in Table 1. It can be seen that the chosen form of wave functions is quite adequate since the calculated oscillator strength values are sufficiently close both to experimental data and to the results obtained by more complex models.

It is obvious that a sufficiently correct calculation of the excitation cross-sections requires complex and laborious calculations with a computer. It is natural therefore to seek a simple calculation method that would give an acceptable accuracy in a number of cases. The semi-empirical formula proposed by Van Regemorter [24] is used widely at present. In the case of cross-section σ and excitation rate $<v\sigma>$ for transition $0 \to 1$ we have, according to Ref. [24], the following expressions:

$$\sigma_{01} = 3.8 \cdot 10^{-16} \cdot f_{01} (\frac{Ry}{\Delta E})^{3/2} \frac{\gamma(u)}{u+1} [cm^2], \qquad (11)$$

$$(v\sigma)_{01} = 3.2 \cdot 10^{-7} f_{01} (\frac{Ry}{\Delta E})^{3/2} \beta^{1/2} e^{-\beta} P(\beta) [\frac{cm^3}{s}]. \qquad (12)$$

Here f_{01} is the oscillator strength for absorption, ΔE is the transition energy, $u \equiv \mathcal{E}/\Delta E - 1$, $\mathcal{E}$ is the incident electron energy and $\beta \equiv \Delta E/T$. The values of function $\gamma(u)$ can be found, for example, in Ref. [7]. For $u \gg 1$

---

[*]   It should be pointed out here that the "Atom" program can be used to
       calculate the cross-sections for both allowed and forbidden and for
       intercombination transitions.

we have: $\gamma(u) \approx 0.27 \ln(1 + u)$. Function $P(\beta)$ for $\beta \ll 1$ has the following asymptotic form: $P(\beta) \approx -\sqrt{3}/2\pi \mathrm{Ei}(-\beta)$. The results of tabulation of $P(\beta)$ for some values of β are given in Table 2 [24].

Table 2

β	$P(\beta)$
0.01	1.16
0.02	0.956
0.04	0.758
0.1	0.493
0.2	0.331
0.4	0.209
1	0.1
2	0.063
4	0.04
10	0.023
> 10	0.066 $\beta^{-1/2}$

In Ref. [7] the excitation cross-sections are represented in the following form:

$$\sigma_{01} = \pi a_0^2 \left(\frac{Ry}{DE}\right)^2 \left(\frac{E_1}{E_0}\right)^{3/2} \frac{Q}{2l_0 + 1} \Phi(u). \quad (13)$$

Here a_0 is the Bohr radius, DE the scale factor (the most frequently used values are DE = ΔE and DE = Z^2Ry; for neutral atoms Z = 1), E_0, E_1 are the energies of the lower (o) and upper (1) level, respectively, reckoned from the ionization limit, l_0 the electron orbital moment in the initial state, Q the so-called angular factor and u = $\mathcal{E}$/DE - 1. In the present study we use the value of DE = 2Ry. Function $\Phi(u)$ has different forms for calculation of the contribution due to the direct and mixed part to the cross-section and for calculation of the contribution due to the exchange part. For function $\Phi'(u)$ (direct and mixed part) we have:

$$\Phi'(u) = \frac{c'}{u + \varphi'} \sqrt{u/(u + \alpha)} . \quad (14)$$

For $\Phi''(u)$ (exchange part) we have:

$$\Phi''(u) = \frac{c''}{(u + \varphi'')(u + 1)^2} \sqrt{u/(u+\alpha)} . \quad (15)$$

where $\alpha = \Delta E/DE$.

12

Consequently, the excitation rates are written in the form:

$$\langle v\sigma \rangle_{01} = 10^{-8} \left(\frac{R_y \cdot E_1}{DE \cdot E_0} \right)^{3/2} \frac{Q}{2I_0 + 1} e^{-\bar{\beta}} G(\beta) \left[\frac{cm^3}{s} \right].$$ (16)

Here $\beta \equiv DE/T$, $\bar{\beta} = \Delta E/T = \beta \Delta E/DE$.

$$G'(\beta) = \frac{A'\beta^{1/2}(1 + \beta)}{\beta + \chi}(1 + \alpha\beta)^{-1/2},$$ (17)

$$G''(\beta) = \frac{A''\beta^{3/2}}{\beta + \chi}(1 + \alpha\beta)^{-1/2}.$$ (18)

The so-called angular factor Q for transitions with $\Delta S = 0$ is equal to one except for excitation from the ground state, where Q = 2. For transitions with $\Delta S = 1$ Q = $(2S_1 + 1)/4$, where S_1 is the spin of the final state. For intercombination transitions with excitation from the ground state Q = 3/2.

It is obviously of interest to compare the results of calculations by the semi-empirical formula of Van Regemorter, by the Coulomb-Born approximation, and also with the available experimental data. A detailed experimental study of the cross-sections for some transitions in the helium atom is contained in Ref. [21]. Table 3 gives the results of Ref. [21] and the results of calculations of <vσ> in the Coulomb-Born approximation for T_e = 3 eV (in units of 10^{-5} cm^3/s) [21].

From the data in Table 3 it can be seen that inclusion of normalization in the Coulomb-Born approximation (which obviously, in the case of the neutral atom, coincides simply with the Born approximation) considerably improves the degree of agreement between the experimental and theoretical results. It is also seen that there is satisfactory agreement between the results of calculation by the single-parameter formula of Van Regemorter (12) and those by the two-parameter formula (16).

We now systematically compare the available data for a number of transitions, including our own calculations (present study).

1. $1^1S_0 - 2^1P$ transition [4, 7, 12-14, 17, 18, 22, 24]. (In the subsequent tables the values of σ are given in cm^2.)

Table 3

Transition	$(v\sigma)_{exp}$ [21]	$(v\sigma)$ [21] CB.)	$(v\sigma)$ [21] with normal-ization	$(v\sigma)$ by formula (12)
3³S – 3³P	1,4 ± 0,3	2,3	1,3	1,2
3¹S – 3¹P	2,4 ± 0,5	3,6	2,4	2,3
2³S – 2³P	0,1 ± 0,02	0,18	0,11	0,06
2¹S – 2¹P	0,2 ± 0,03	0,38	0,25	0,15

*) CB – Coulomb-Born approximation

Table 3A

ϵ, eV	[8]$_{exp}$	[11]	[14]	[18]	Present study	[24]
40	$7,7.10^{-18}$	$7,6.10^{-17}$	—	$5,5.10^{-18}$	$10,7.10^{-18}$	$9,8.10^{-18}$
102	$1,0.10^{-17}$	$1,4.10^{-17}$	$1,36.10^{-17}$	$8,0.10^{-18}$	$8,5.10^{-18}$	$7,9.10^{-18}$

Table 3B

ϵ, eV	[9]$_{exp}$	[15]	[18]	Present study	[24]
20	6.10^{-17}	4.10^{-17}	$7,5.10^{-17}$	$9,9.10^{-17}$	
15,3	—	$2,6.10^{-17}$	—	$3,5.10^{-17}$	$1,17.10^{-17}$

Table 3C

ϵ, eV	[8]$_{exp}$	[13]	[14]	Present study	[24]
40	$1,57.10^{-18}$	—	$5,3.10^{-18}$	$4,4.10^{-18}$	3.10^{-18}
50	2.10^{-18}	7.10^{-18}	—	$4,7.10^{-18}$	4.10^{-18}

Table 3D

ϵ, eV	[10]$_{exp}$	[24]
50	$3,37.10^{-19}$	$1,38.10^{-17}$

From the data given in the table, it can be seen that the theoretical results agree satisfactorily with each other and with the experimental data, except the result of Ref. [11] for ϵ = 40 eV, which differs from the remaining results by a factor of about 8-10.

2. $2^3S - 3^3P$ transition [9, 15, 18, 24].

3. $2^3S - 2^3P$ transition [12, 15, 17, 18, 24].

4. $2^3S - 4^3P$ transition [15, 18, 24].

5. $1^1S_o - 3^1P$ transition [8, 14, 18, 22, 24].

6. 1^1S_0 - 4^1P transition [18, 22, 24].

7. 2^1S - 2^1P transition [1, 12, 14, 17, 18, 21, 24].

8. 2^1S - 3^1P transition [15, 18, 21, 24].

9. 2^1S - 4^1P transition [15, 18, 24].

10. 2^1P - 3^1S transition [10, 24].

It can be seen that for the 2^1P - 3^1S transition there is a huge discrepancy (a factor of ~40) between experimental data and the results of calculations by the Van Regemorter formula. Since there are no grounds at present to doubt that the Van Regemorter formula satisfactorily describes the cross-sections (with an accuracy of ~2-3), the result given in Ref. [10] appears to be erroneous.

2.2   Forbidden and intercombination transitions

The data for the forbidden and intercombination transitions are contained in the following sources:

(a)   Transitions from the ground state in Refs [1, 9, 11, 15, 17-20, 25-31, 32];

(b)   Transitions between excited states in Refs [1, 9, 12, 14, 17, 18, 31, 33-35].

The experimental data are given in Refs [9, 25, 29, 34], while the remaining studies contain the results of calculations using various approximations (Coulomb-Born approximation, the R-matrix method and the distorted wave method). Thus, a modification of the distorted wave method was used in Ref. [26] to calculate the cross-sections in the $25 < \mathcal{E} \le 150$ eV region. The results of calculation of cross-sections for a number of transitions in the $21.4 < \mathcal{E} \le 30$ eV and $80 < \mathcal{E} < 200$ eV regions by the R-matrix formalism are given in Refs [11, 12, 28]. In Refs [13, 14, 27] the cross-section calculations were performed by the distorted wave method in the 30-300 eV region. It should be noted that this method is most successful in the calculation of the excitation cross-section for level 2^3S. The analysis

carried out in Ref. [14] shows that in the case of the excitation cross-section for level 2^1S the difference between the theoretical and experimental data in the 50-200 eV region can be reduced if the contribution of the pseudostates is taken into account. The diagram formalism of the many-body theory was used in Ref. [30] to calculate the excitation cross-sections for triplet levels in the 30-250 eV region. In Ref. [32] the excitation cross-section for 3^3D was calculated with the use of the Oppenheimer approximation. According to the opinion expressed in Ref. [29], this approximation ensures better agreement with experimental data than the approximation used in Ref. [16]. In Ref. [15] the excitation cross-section was calculated in the Born approximation and with the use of the Vainshtein-Presnyakov-Sobelman approximation (see, for example, Ref. [22]). In Ref. [33] the Glauber approximation was used and some results of other authors were compared.

We now compare the existing data for the transitions of interest.

A.   Transitions from the ground state

1. 1^1S_o - 2^1S transition [1, 11, 12, 14, 17, 18, 20, 25-27].

It should be noted that the data given in the different studies differ from each other (this applies to both experimental and theoretical results). Thus, for $\varepsilon = 29.6$ eV, according to Ref. [25], $\sigma = 6 \times 10^{-18}$ cm^2, but according to Ref. [11], $\sigma = 2.2 \times 10^{-18}$ cm^2. Since the available experimental data are very scarce (there are data only for two values of incident electron energy in Ref. [11] and for three values in Ref. [25]), we have to rely on the calculations, which agree with each other and with the available experimental data.

Table 4 gives such "averaged" cross-sections for several values of ε, eV. For comparison, we give the results of calculations by the "Atom" program: $\sigma(\varepsilon = 30) = 7.3 \times 10^{-18}$ cm^2, $\sigma(52) = 5 \times 10^{-18}$ cm^2, $\sigma(100) = 2.4 \times 10^{-18}$ cm^2.

Table 4

ε, eV	σ, 10^{-18} cm^2
22	1.2
25	2.6
30	5.2
39	5.2
52	4.4
60	2.6
80	2.1
100	1.8

Table 5

T, eV	$\langle v\sigma \rangle$, cm^3 s^{-1}	
	calc. by "Atom" program	[20]
0.43	$3.5.10^{-20}$	$6.4.10^{-20}$
0.65	$3.8.10^{-13}$	$6.3.10^{-13}$
0.86	$8.8.10^{-16}$	13.10^{-16}
1.72	$1.4.10^{-14}$	$1.74.10^{-14}$
2.6	$7.8.10^{-13}$	$8.6.10^{-13}$
4.3	$1.7.10^{-11}$	$1.7.10^{-11}$

Table 5 presents the calculation results for $\langle v\sigma \rangle$ by the "Atom" program obtained in Ref [20]. It can be seen that the strong coupling method gives approximately the same results as the Born approximation, when the exchange effects are included and the normalization is performed.

2. $1^1S_0 - 3^1S$ transition [1, 14, 22, 27].

There are no experimental data for this transition. The calculation results given in Refs [14, 27] differ from each other by a factor of about 2-3 (thus for ε = 50 eV, according to Ref. [14], we have $\sigma = 0.84 \times 10^{-18}$ cm^2, whereas, according to Ref. [23], $\sigma = 0.298 \times 10^{-18}$ cm^2).

3. $1^1S_0 - 4^1S$ transition [1, 22].

4. $1^1S_0 - 2^3S$ transition [1, 12, 14, 17, 20, 22, 25, 27-29, 31].

The experimental data for ε = 29.6 eV and 40.1 eV are given in Ref. [25] and those for ε = 20 eV in Ref [29]. The remaining studies contain the results of calculations using different approximations. Table 6 compares the results given in the various sources.

Table 6

ε, eV	$\sigma, \pi a_0^2$							
	[25]exp	[29]exp	[12]	[13]	[17]	[28]	[30]	[31]exp
20	—	$7.2.10^{-3}$	$9.9.10^{-3}$	—	3.10^{-3}	$4.8.10^{-3}$	—	$2.8.10^{-3}$
30	$8.0.10^{-3}$	—	$5.6.10^{-3}$	$3.8.10^{-3}$	$1.5.10^{-3}$	$4.8.10^{-3}$	—	—
40	—	—	—	$1.8.10^{-3}$	$0.8.10^{-3}$	—	$2.2.10^{-3}$	$2.3.10^{-3}$
60	—	—	—	$4.6.10^{-3}$	—	—	$6.4.10^{-3}$	—
80	—	—	—	$3.1.10^{-3}$	2.10^{-3}	$5.3.10^{-3}$	$3.8.10^{-3}$	—
100	—	—	$2.3.10^{-3}$	$2.2.10^{-3}$	—	$2.3.10^{-3}$	$2.2.10^{-3}$	—

The values of σ and $\langle v\sigma \rangle$ are given in Ref. [18] and they agree to a satisfactory degree with the experimental data at low energies. Thus, for $\mathcal{E} = 20$ eV, according to Ref. [18], $\sigma = 2.8 \times 10^{-2} \pi a_o^2$ and, according to Ref. [31], $\sigma_{exp} = 2.8 \times 10^{-2} \pi a_o^2$.

5. $1^1S_o - 3^3S$ transition [18, 22].

The results of calculation of $\langle v\sigma \rangle$ given in Ref. [18] differ from the values obtained by the "Atom" program in the low-temperature region ($T_e < 40$ eV) by a factor of about 1.5. In the high-temperature region the decrease in σ and $\langle v\sigma \rangle$, according to Ref. [18], occurs much more slowly than that according to Ref. [22].

6. $1^1S_o - 4^3S$ transition [18, 22].

The comments on the preceding transition apply equally to this transition.

7. $1^1S_o - 2^3P$ transition [1, 12, 17-19, 22, 28].

Since there are no experimental data, we confine ourselves to comparing the results of the various calculations (Table 7).

Table 7

ϵ, eV	Source	σ, πa_o^2
28.6	[29]	$6.8.10^{-2}$
30	[18]	$2.5.10^{-2}$
30	[1]	$2.8.10^{-2}$
32.4	[17]	$1.76.10^{-1}$
40	[1]	$1.76.10^{-2}$
40	[17]	$1.38.10^{-1}$
40	[18]	$3.4.10^{-2}$
80	[1]	$2.8.10^{-3}$
80	[17]	$2.8.10^{-2}$
80	[18]	$2.2.10^{-2}$
81.6	[28]	10^{-2}
82.5	[12]	$3.8.10^{-3}$
100	[1]	$1.7.10^{-3}$
100	[12]	$1.8.10^{-3}$
100	[28]	$3.7.10^{-3}$

The results of calculation, for example, for $T_e = 40$ eV by the "Atom" program show good agreement with the results of Ref. [18]. The following empirical formula for σ is given in Ref. [1]:

$$\sigma(x) = 0.18 \, \pi a_0^2 \, (\frac{1}{x^3} - \frac{1}{x^5}),$$ (19)

where $x = \mathcal{E} / \Delta E$.

The comparison of the values of $\langle v\sigma \rangle$ obtained by formula (19) and those by the "Atom" program shows sufficiently good agreement.

8. $1\,{}^1S_0 - 3\,{}^3P$ transition [18, 22].

The results of Ref. [18] and those obtained by the "Atom" program agree satisfactorily with each other. Thus, for $T_e = 40$ eV, according Ref. [18], we have $\langle v\sigma \rangle = 1.7 \times 10^{-10}$ cm^3/s, while the "Atom" program gives $\langle v\sigma \rangle = 1.8 \times 10^{-10}$ cm^3/s; for $T_e = 100$ eV we have, respectively, 9×10^{-11} cm^3/s and 9.7×10^{-11} cm^3/s.

9. $1\,{}^1S_0 - 4\,{}^3P$ transition [22].

10. $1\,{}^1S_0 - 3\,{}^3D$ transition [31].

11. $1\,{}^1S_0 - 4\,{}^3D$ transition [22].

B.   Transitions between excited states

1. $2\,{}^1S - 3\,{}^1S$ transition [1, 15, 17].

The cross-section calculation results given in Refs [15, 17] differ by a factor of 2-3. Unfortunately, the formula given in Ref. [1] contains undetermined parameters so that it cannot be used directly.

2. $2\,{}^1S - 3\,{}^1D$ transition [1, 15, 17].

3. $2\,{}^1S - 2\,{}^3S$ transition [1, 12, 17, 18].

It should be pointed out that the results of all calculations (experimental data do not exist) agree well with each other in the low-energy region, but in the region of fairly high energies (~100 eV) there is a very strong discrepancy (by a factor of up to 10-100) between the results of Ref. [18], obtained on the basis of the semi-empirical formula proposed in Ref. [1], and those of our calculations by the "Atom" program. Figure 2 shows the dependences of $\langle v\sigma \rangle$ on T_e, which were calculated by the two methods.

As to this discrepancy, we should point out the following. The cross-sections for intercombination transitions with $\Delta S = 1$ should decrease asymptotically,
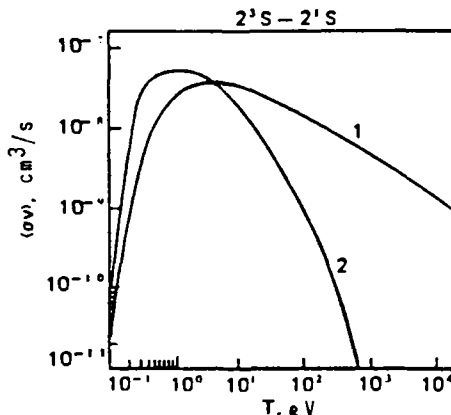
Fig. 2. Dependence of the excitation rate for the 2^1S-2^3S transition on T_e: 1 - [18]; 2 - present study.

for large $\mathcal{E}$, as $\mathcal{E}^{-3}$. In the cross-sections calculated by us this behaviour takes place automatically. The reason for the discrepancy with Ref. [18] is not at all clear at present and, therefore, the latter's data for this transition are doubtful. Some slowing down of the decrease in the cross-section for moderate energies could indeed be produced by effects of a strong coupling with the $2^3L - 2^3L''$ channel. But at high energies the law $\sigma \sim 1/\mathcal{E}^3$ should be preserved. At present, detailed calculations of this effect are not known to us.

4. $2^1S - 2^3P$ transition [1, 12, 17-19].

The comments made on the preceding transition are also valid for this transition.

5. $2^3S - 2^1P$ transition [12, 17-19].

The calculation results of Ref. [17] show good agreement with the data of Ref. [18] for low temperatures.

6. $2^1P - 2^3P$ transition [12, 17-19].

It should be pointed out that the results of Refs [12, 17] for $\mathcal{E} = 100$ eV differ by an order from those of Ref. [18] but are close to each other. Table 8 compares the values of $<v\sigma>$, cm^3/s, taken from Ref. [19] and those obtained by the "Atom" program.

Table 8

Transition	Calculation method	T, eV							
		0,086	0,17	0,43	0,65	0,86	1,72	2,6	4,3
$2^1P - 2^3P$	[19]	$3{,}3.10^{-1}$	$1{,}3.10^{-1}$	$2{,}7.10^{-1}$	$3{,}11.10^{-1}$	$3{,}15.10^{-1}$	$2{,}8.10^{-1}$	$2{,}5.10^{-1}$	$19{,}5.10^{-2}$
	"Atom"	$2{,}7.10^{-1}$	10^{-1}	$1{,}9.10^{-1}$	$1{,}96.10^{-1}$	$1{,}89.10^{-1}$	$1{,}5.10^{-1}$	$1{,}28.10^{-1}$	$8{,}9.10^{-2}$

7. $2^3S - 3^3S$ transition [15-28].

Comparison of the calculation results (experimental data are lacking) shows that calculations by the "Atom" program give values differing by a factor of 2-3 from those presented in Refs [15, 28].

8. $2^3S - 3^3D$ transition [1, 9, 15].

Comparison of experimental data [9] with calculation results [1, 15] shows that for $\mathcal{E} = 10$ eV calculation gives cross-section values lower by a factor of 3-4 than the experimental data but for $\mathcal{E} = 20$ eV the results exhibit sufficiently good agreement.

9. $2^3S - 4^3D$ transition [8, 9].

The results of calculation by the "Atom" program agree satisfactorily with experimental data [9] in the $\mathcal{E} = 3$-20 eV region. Thus, for $\mathcal{E} = 20$ eV, according to Ref. [9], we have $\sigma = 2.3 \times 10^{-17}$ cm^2, while our calculation gives $\sigma = 2.2 \times 10^{-17}$ cm^2.

10. $2^3S - 3^1P$ transition [9, 34].

The results of experiment [9] and calculation [34] show satisfactory agreement with each other. Thus for $\mathcal{E} = 10$ eV $\sigma_{exp} = 10^{-17}$ cm^2 and $\sigma_{theor} = 1.8 \times 10^{-17}$ cm^2. The calculation results of Ref. [34] are presented in Table 9.

11. $4^1P - 4^3D$ transition [33].

The experimental data for $\quad = 4.65$ eV are contained in Ref. [33].

12. $2^3S - 3^1D$ transition [34].

13. $2^3S - 4^1S$ transition [34].

14. $2^3S - 4^1P$ transition [34].

Table 9

ε, eV	σ, πa_0^2
4	2.1
5	1.5
6	0.94
8	0.41
10	0.21
15	0.063
20	0.027
30	8.10^{-3}
40	3.10^{-3}
50	$1.7.10^{-3}$
100	10^{-3}

Table 10

ε, eV	Transition				
	$2^3S - 3^1D$	$2^3S - 4^1S$	$2^3S - 4^1P$	$2^3S - 4^1D$	$2^3S - 3^1S$
3	—	—	—	—	0.44
4	3.2	—	0.26	0.62	3.2
5	2	0.15	0.46	0.77	1.9
6	1.2	0.14	0.32	0.5	1.2
8	0.52	0.11	0.15	0.22	0.52
10	0.26	0.083	0.076	0.11	0.28
15	0.078	0.039	0.023	0.034	0.092
20	0.033	0.021	$9.6.10^{-3}$	0.014	0.043
30	0.0097	$7.6.10^{-3}$	$2.9.10^{-3}$	$4.2.10^{-3}$	0.014
40	$4.2.10^{-3}$	$3.6.10^{-3}$	$1.2.10^{-3}$	$1.8.10^{-3}$	$6.5.10^{-3}$
50	$2.1.10^{-3}$	$1.9.10^{-4}$	$6.2.10^{-4}$	$9.1.10^{-4}$	$3.5.10^{-3}$
70	$7.7.10^{-4}$	$7.6.10^{-4}$	$2.3.10^{-4}$	$3.3.10^{-4}$	$1.3.10^{-3}$
100	$2.6.10^{-4}$	$3.7.10^{-4}$	$7.8.10^{-5}$	$1.1.10^{-4}$	$4.7.10^{-4}$

15. $2^3S - 4^1D$ transition [34].

16. $2^3S - 3^1S$ transition [34].

Table 10 gives the values of σ, πa_0^2, calculated in Ref. [34]

for some values of incident electron energy.

2.3 Recommended excitation rates

Thus, from the foregoing discussions of available data on the

electron-impact excitation cross-sections for the various levels of He, it can

be concluded that the results of calculations by the "Atom" program are in

sufficiently good agreement with the existing experimental data. In cases

where experimental data are lacking there is quite reasonable agreement (to

within a factor of 1.5-2) between the results of calculations by the "Atom"

code and those by the strong coupling method (taking into account various

numbers of states). This code was used, therefore, to calculate the

cross-sections and to determine parameters A and χ entering into forumlae

(17) and (18). These parameters are given in Table 11. We give some

explanations about this table. The first column gives the transition

(1S - 2P, 2P - 3D and so on) and the second column the multiplicity of the

initial and final states. The third column contains the value of k = $|l_0 - l_1|$.

The fourth and fifth columns give the energies of the initial and final states

Table 11   Approximation parameters

TR	SS	K	E0	E1	F	A/X
1S-2P	11	1	1.8072	0.2506	1.55E-01	4.28E+01/0.95
1S-2P	11	1	1.8072	0.2663	2.00E-01	4.35E+00/1.72
1S-2S	13	0	1.8072	0.3154	3.23E-10	3.96E+00/1.00
1S-2S	19	0	1.8072	0.3154	3.23E-10	3.53E+00/0.45
1S-3D	11	2	1.8072	0.1112	9.51E-02	9.07E-01/0.23
1S-3D	13	2	1.8072	0.1113	9.53E-02	3.19E-01/2.09
1S-3P	11	1	1.8072	0.1113	9.09E-02	1.07E+01/0.06
1S-3P	13	1	1.8072	0.1162	9.81E-02	1.01E+01/1.78
1S-3S	13	0	1.8072	0.1290	8.76E-10	4.05E+00/1.07
1S-3S	19	0	1.8072	0.1290	8.76E-10	2.56E+00/0.42
1S-4D	11	2	1.8072	0.0626	2.32E-02	5.07E-01/0.22
1S-4D	13	2	1.8072	0.0626	2.33E-02	9.35E-01/2.11
1S-4F	11	3	1.8072	0.0625	1.55E-02	9.84E-03/0.38
1S-4F	13	3	1.8072	0.0625	1.55E-02	9.01E-03/2.33
1S-4P	11	1	1.8072	0.0626	1.66E-02	1.01E+01/0.06
1S-4P	13	1	1.8072	0.0646	1.88E-02	1.08E+01/1.81
1S-4S	13	0	1.8072	0.0698	3.13E-10	4.08E+00/1.10
1S-4S	19	0	1.8072	0.0698	3.13E-10	2.32E+00/0.41
2P-2P	31	0	0.2663	0.2506	2.67E-02	3.65E+01/2.12
2P-3D	11	1	0.2506	0.1112	2.08E+00	9.33E+02/0.11
2P-3D	13	1	0.2506	0.1113	2.08E+00	2.67E+02/8.01
2P-3D	31	1	0.2663	0.1113	1.83E+00	2.71E+02/8.34
2P-3D	33	1	0.2663	0.1113	1.83E+00	7.89E+02/0.12
2P-3P	13	0	0.2506	0.1162	1.60E-03	5.80E+01/5.12
2P-3P	19	0	0.2506	0.1113	1.08E-08	1.42E+02/0.50
2P-3P	31	0	0.2663	0.1113	1.51E-03	9.72E+01/3.82
2P-3P	31	0	0.2663	0.1113	1.51E-03	9.72E+01/3.82
2P-3P	39	0	0.2663	0.1162	1.19E-08	1.31E+02/0.50
2P-3P	39	0	0.2663	0.1162	1.19E-08	1.31E+02/0.50
2P-3S	13	1	0.2506	0.1374	2.83E-01	1.58E+01/4.37
2P-3S	31	1	0.2663	0.1225	7.97E-02	3.24E+01/6.79
2P-3S	33	1	0.2663	0.1374	2.07E-01	7.40E+01/0.12
2P-4D	11	1	0.2506	0.0626	3.65E-01	4.28E+02/0.22
2P-4D	13	1	0.2506	0.0626	3.65E-01	3.15E+02/9.75
2P-4D	31	1	0.2663	0.0626	3.70E-01	3.15E+02/9.87
2P-4D	33	1	0.2663	0.0626	3.70E-01	3.99E+02/0.21
2P-4F	11	2	0.2506	0.0625	3.08E+01	1.08E+02/0.64
2P-4F	13	2	0.2506	0.0625	3.08E+01	4.30E+02/24.7
2P-4F	31	2	0.2663	0.0625	2.79E+01	3.80E+02/25.4
2P-4F	33	2	0.2663	0.0625	2.79E+01	8.17E+01/0.62
2P-4P	13	0	0.2506	0.0646	4.82E-03	8.38E+01/7.19
2P-4P	19	0	0.2506	0.0626	3.58E-08	9.23E+01/0.43
2P-4P	31	0	0.2663	0.0626	4.89E-08	6.58E+01/5.37
2P-4P	39	0	0.2663	0.0647	2.65E-02	8.72E+01/0.76
2P-4S	11	1	0.2506	0.0672	2.38E-02	1.60E+01/0.14
2P-4S	13	1	0.2506	0.0730	3.82E-02	1.76E+01/5.29
2P-4S	31	1	0.2663	0.0672	1.56E-02	4.10E+01/8.81
2P-4S	33	1	0.2663	0.0730	3.15E-02	2.19E+01/0.15
2S-2P	11	1	0.2919	0.2506	8.34E-02	8.34E+01/0.19
2S-2P	13	1	0.2919	0.2663	1.92E-01	2.24E+01/3.10
2S-2P	31	1	0.3505	0.2506	6.81E-01	3.84E+01/3.24
2S-2P	33	1	0.3505	0.2663	8.34E-01	3.02E+02/0.16
2S-2S	31	0	0.3505	0.2919	5.40E-02	1.77E+01/3.47
2S-3D	11	2	0.2919	0.1112	5.34E+01	1.53E+02/0.77
2S-3D	13	2	0.2919	0.1113	5.34E+01	2.00E+02/10.3
2S-3D	31	2	0.3505	0.1112	3.18E+01	1.68E+02/9.18
2S-3D	33	2	0.3505	0.1113	3.19E+01	1.05E+02/0.75
2S-3P	11	1	0.2919	0.1113	1.68E-01	9.08E+01/9.85
2S-3P	13	1	0.2919	0.1113	1.32E-01	1.25E+01/0.06
2S-3P	31	1	0.3505	0.1113	2.24E-02	2.97E+01/4.30
2S-3P	33	1	0.3505	0.1162	6.37E-02	1.76E+01/0.14
2S-3S	13	0	0.2919	0.1374	4.62E-03	9.61E+00/5.28
2S-3S	19	0	0.2919	0.1229	8.70E-09	4.38E+01/0.66
2S-3S	31	0	0.3505	0.1225	3.92E-03	2.47E+01/6.89
2S-3S	39	0	0.3505	0.1374	1.10E-08	3.53E+01/0.68
2S-4D	11	2	0.2919	0.0626	4.62E+00	7.80E+01/0.96
2S-4D	13	2	0.2919	0.0626	4.60E+00	2.08E+02/11.8
2S-4D	31	2	0.3505	0.0626	5.08E+00	1.74E+02/9.65
2S-4D	33	2	0.3505	0.0626	5.07E+00	6.86E+01/0.87
2S-4F	11	3	0.2919	0.0625	1.96E+03	2.27E+01/1.03
2S-4F	13	3	0.2919	0.0625	1.96E+03	2.08E+02/24.3
2S-4F	31	3	0.3505	0.0625	6.77E+02	1.09E+02/19.9
2S-4F	33	3	0.3505	0.0625	6.77E+02	1.15E+01/1.02
2S-4P	11	1	0.2919	0.0625	5.52E+02	2.53E+01/0.06
2S-4P	13	1	0.2919	0.0646	7.45E-02	9.25E+01/9.28
2S-4P	31	1	0.3505	0.0626	1.18E-02	3.10E+01/4.99
2S-4P	33	1	0.3505	0.0646	2.55E-02	1.26E+01/0.11
2S-4S	13	0	0.2919	0.0730	1.24E-03	1.16E+01/6.76
2S-4S	19	0	0.2919	0.0674	9.68E-09	2.50E+01/0.81
2S-4S	31	0	0.3505	0.0672	1.29E-03	2.65E+01/8.05

23

Table 11 (continued)

TR	SS	K	E0	E1	F	A/X
2S-4S	39	0	0.3505	0.0731	3.7AE-09	2.12E+01/0.R3
3D-3D	31	0	0.1113	0.1112	1.37E-04	1.27E+02/4.12
3D-4D	13	0	0.1113	0.0626	3.14E-09	1.69E+02/8.96
3D-4D	18	0	0.1113	0.0636	3.05E-09	1.89E+02/0.35
3D-4D	31	0	0.1113	0.0626	1.60E-07	1.66E+02/8.96
3D-4D	39	0	0.1113	0.0626	2.69E-09	4.97E+02/0.35
3D-4F	11	1	0.1113	0.0625	5.07E+00	5.57E+03/0.11
3D-4F	13	1	0.1113	0.0625	5.07E+00	4.52E+02/13.6
3D-4F	31	1	0.1113	0.0625	5.07E+00	4.52E+02/13.6
3D-4F	33	1	0.1113	0.0625	5.07E+00	5.57E+03/0.11
3D-4P	11	1	0.1113	0.0626	5.62E-02	1.10E+02/0.33
3D-4P	13	1	0.1113	0.0646	1.12E-01	2.02E+02/16.0
3D-4P	31	1	0.1113	0.0626	5.59E-02	1.61E+02/14.0
3D-4P	33	1	0.1113	0.0646	1.11E-01	1.47E+02/0.22
3D-4S	11	2	0.1113	0.0672	3.A4E+01	3.43E+01/0.74
3D-4S	13	2	0.1113	0.0730	6.10E+01	2.11E+01/9.A2
3D-4S	31	2	0.1113	0.0672	3.A8E+01	1.63E+01/8.27
3D-4S	33	2	0.1113	0.0730	6.09E+01	6.0AE+01/0.77
3P-3D	11	1	0.1113	0.1112	5.51E-03	1.04E+04/0.37
3P-3D	13	1	0.1113	0.1113	3.67E-03	3.7AE+01/4.13
3P-3D	31	1	0.1162	0.1112	3.39E-01	3.71E+01/4.05
3P-3D	33	1	0.1162	0.1113	3.36E-01	5.17E+03/0.28
3P-3D	31	0	0.1162	0.1113	1.43E-02	2.81E+01/3.44
3P-4D	11	1	0.1113	0.0626	1.85E+00	1.94E+03/0.14
3P-4D	13	1	0.1113	0.0626	1.85E+00	8.49E+01/10.7
3P-4D	33	1	0.1162	0.0626	1.43E+00	1.37E+02/13.6
3P-4D	33	1	0.1162	0.0626	1.43E+00	1.35E+02/13.5
3P-4F	11	2	0.1113	0.0625	8.12E+02	1.21E+03/0.69
3P-4F	13	2	0.1113	0.0625	8.12E+02	8.52E+02/23.5
3P-4F	31	2	0.1162	0.0625	7.52E+02	1.01E+03/23.5
3P-4F	33	2	0.1162	0.0625	7.52E+02	1.14E+03/0.69
3P-4P	13	0	0.1162	0.0646	6.24E-04	1.0AE+02/13.2
3P-4P	17	0	0.1113	0.0626	8.87E-09	4.44E+02/0.44
3P-4P	31	0	0.1162	0.0625	5.4AE-04	1.07E+02/12.2
3P-4P	39	0	0.1162	0.0647	4.66E-09	4.17E+02/0.44
3P-4S	11	1	0.1113	0.0672	2.81E-01	2.72E+02/0.14
3P-4S	13	1	0.1113	0.0730	5.73E-01	2.76E+01/10.5
3P-4S	31	1	0.1162	0.0672	1.79E-01	2.17E+01/13.0
3P-4S	33	1	0.1162	0.0730	4.35E-01	4.59E+01/0.16
3S-3D	11	2	0.1225	0.1112	4.2AE+01	1.49E+02/0.47
3S-3D	13	2	0.1225	0.1113	4.27E+01	2.03E+01/4.50
3S-3D	31	2	0.1374	0.1112	8.52E+01	3.36E+01/4.62
3S-3D	33	2	0.1374	0.1113	8.59E+01	1.77E+02/0.48
3S-3D	33	2	0.1374	0.1113	8.69E+01	1.05E+03/8.28
3S-3P	13	1	0.1225	0.1162	3.06E-01	4.34E+00/3.30
3S-3P	31	1	0.1374	0.1113	1.10E+00	1.33E+01/3.97
3S-3P	33	1	0.1374	0.1162	8.90E-01	2.16E+03/0.19
3S-3S	31	0	0.1374	0.1225	1.37E-02	5.64E+01/3.69
3S-4D	11	2	0.1225	0.0626	2.43E+02	2.14E+02/0.67
3S-4D	13	2	0.1225	0.0626	2.43E+02	3.27E+01/10.5
3S-4D	31	2	0.1374	0.0626	1.24E+02	4.99E+01/13.3
3S-4D	33	2	0.1374	0.0626	1.24E+02	9.67E+01/0.60
3S-4F	11	3	0.1225	0.0625	1.09E+05	2.03E+02/0.89
3S-4F	13	3	0.1225	0.0625	1.09E+05	1.75E+02/17.6
3S-4F	31	3	0.1374	0.0625	7.56E+04	1.69E+02/17.0
3S-4F	33	3	0.1374	0.0625	7.56E+04	1.74E+02/0.91
3S-4P	11	1	0.1225	0.0626	1.68E-01	1.16E+02/0.10
3S-4P	13	1	0.1225	0.0646	2.90E-01	1.49E+01/10.9
3S-4P	31	1	0.1374	0.0626	1.11E-02	2.07E+01/9.10
3S-4P	33	1	0.1374	0.0646	5.01E-02	5.97E+01/0.28
3S-4S	13	0	0.1225	0.0730	1.55E-03	6.24E+00/9.57
3S-4S	19	0	0.1225	0.0672	2.57E-04	1.31E+02/0.58
3S-4S	31	0	0.1374	0.0672	1.18E-03	9.51E+00/9.48
3S-4S	39	0	0.1374	0.0731	3.06E-04	1.11E+02/0.59
4D-4D	31	0	0.0626	0.0626	9.11E-05	2.62E+01/4.26
4D-4F	11	1	0.0626	0.0625	1.35E-02	3.90E+04/0.38
4D-4F	13	1	0.0626	0.0625	1.30E-02	1.61E+01/4.91
4D-4F	31	1	0.0626	0.0625	1.81E-02	1.62E+01/4.92
4D-4F	33	1	0.0626	0.0625	1.81E-02	3.75E+04/0.38
4F-4F	31	0	0.0625	0.0625	9.39E-07	2.96E+01/4.67
4P-4D	11	1	0.0626	0.0626	1.57E-02	4.40E+04/0.38
4P-4D	13	1	0.0626	0.0626	1.05E-02	1.36E+01/4.56
4P-4D	31	1	0.0646	0.0626	6.10E-01	1.23E+01/4.47
4P-4D	33	1	0.0646	0.0626	6.05E-01	2.38E+04/0.31
4P-4F	11	2	0.0626	0.0625	5.24E+00	5.33E+02/0.48
4P-4F	13	2	0.0626	0.0625	5.23E+00	1.27E+01/5.04
4P-4F	31	2	0.0646	0.0625	1.07E+02	1.14E+01/4.95
4P-4F	33	2	0.0646	0.0625	1.07E+02	8.09E+02/0.48
4P-4P	31	0	0.0646	0.0626	6.04E-03	9.02E+00/3.74
4S-4D	11	2	0.0672	0.0626	2.51E+02	6.23E+02/0.48

Table 11 (continued)

TR	SS	K	E0	E1	F	A/X
4S-4D	13	2	0.0672	0.0626	2.50E+02	2.95E+00/0.26
4S-4D	13	2	0.0672	0.0626	2.50E+02	2.95E+00/0.26
4S-4D	31	2	0.0730	0.0626	4.90E+02	5.29E+00/0.02
4S-4D	33	2	0.0730	0.0626	8.93E+02	6.77E+02/0.48
4S-4F	11	3	0.0672	0.0625	6.27E+04	8.81E+01/0.09
4S-4F	13	3	0.0672	0.0625	6.27E+04	9.46E+00/5.49
4S-4F	31	3	0.0730	0.0625	1.25E+05	1.55E+01/5.62
4S-4F	33	3	0.0730	0.0625	1.25E+05	1.13E+02/0.50
4S-4P	11	1	0.0672	0.0626	7.76E-01	1.15E+04/0.28
4S-4P	13	1	0.0672	0.0646	4.15E-01	3.16E-01/2.64
4S-4P	31	1	0.0730	0.0626	1.48E+00	2.51E+00/4.11
4S-4P	33	1	0.0730	0.0646	1.21E+00	8.60E+03/0.24
4S-4S	31	0	0.0730	0.0672	5.39E-03	7.81E-01/3.48

(E_0, E_1) in Ry, reckoned from the ionization limit. The sixth column presents the value of F. The relationship between the oscillator strength f of the electrical 2k-pole transition and the F value presented in the table (for transitions from 1S F should be doubled) is given by:

$$(2l_0 + 1)f = \frac{k+1}{2^{2k-1}k[(2k-1)!!]^2}\left(\frac{\Delta\epsilon}{137}\right)^{2k-2}F, \qquad (20)$$

where $k = |l_0 - l_1|$ and Δ is the energy of transition in Ry. It can be seen that for dipole transitions (k = 1) the value given in the table is the invariant quantity $(2l_0 + 1)f$ (with respect to the direction of transition). The seventh column contains the values of A and χ. The set of values of A and χ together with formulae (16)-(18) forms a system of data which can be recommended for calculation of the electron-impact level excitation rates for the helium atom in the group with n = 1 to 4. It should be noted that the error of the approximation formulae in most cases does not exceed 25%. Figures 3-20 give the excitation rates, calculated by the "Atom" program, for various transitions in the helium atom.
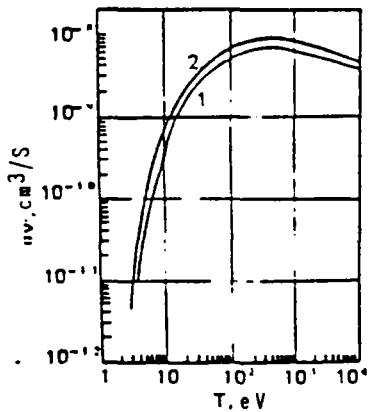
Fig. 3. Dependence of the
excitation rate for the 1^1S-2^1P
transition on T_e: 1-[18];
2 - present study.
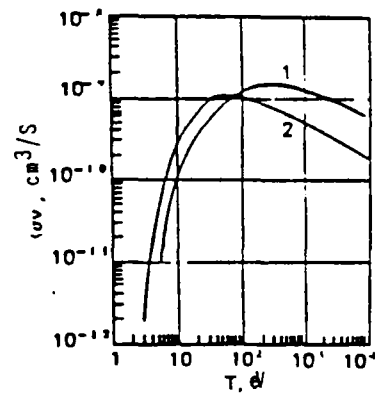
Fig. 4. Dependence of the
excitation rate for the 1^1S-2^1S
transition on T_e: 1-[18]; 2 - present study.
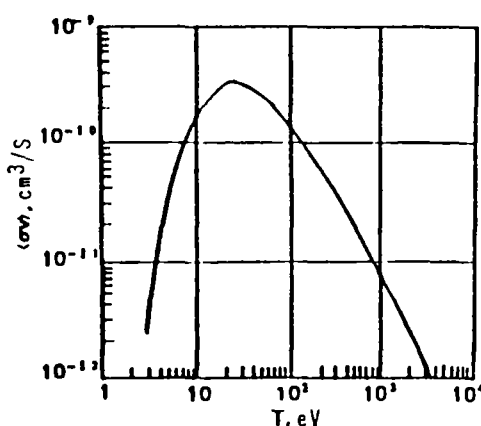
Fig. 5. Dependence of the excitation
rate for the 1^1S-2^3S transition on T_e.
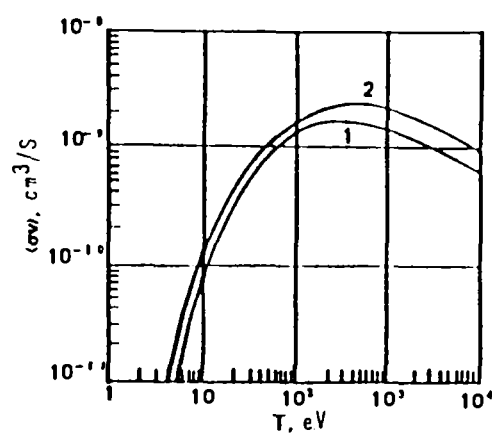
Fig. 6. Dependence of the excitation
rate for the 1^1S-3^1P transition on
T_e: 1-[18]; 2 - present study.
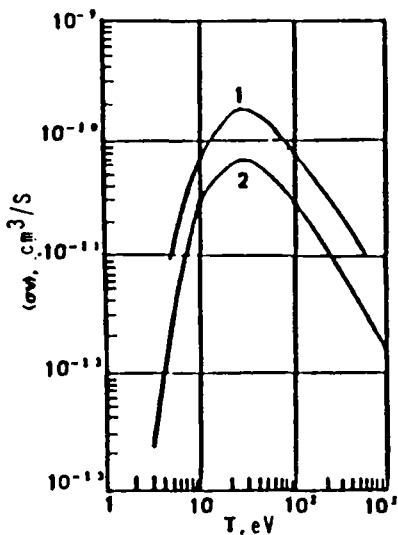
Fig. 7. Dependence of the
excitation rate for the 1^1S-3^3P
transition on T_e: 1-[18];
2 - present study.
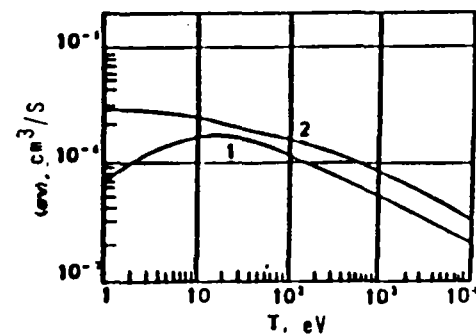
Fig. 8. Dependence of the excit-
ation rate for the 2^1S-2^1P transition
on T_e: 1-[18]: 2 - present study.
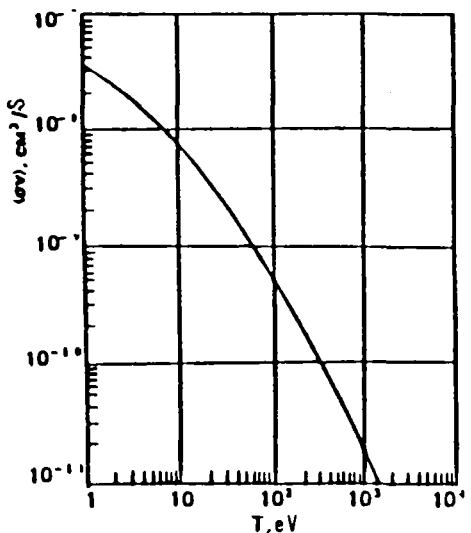
Fig. 9. Dependence of the excitation rate for the 2^3P-2^1P transition on T_e.
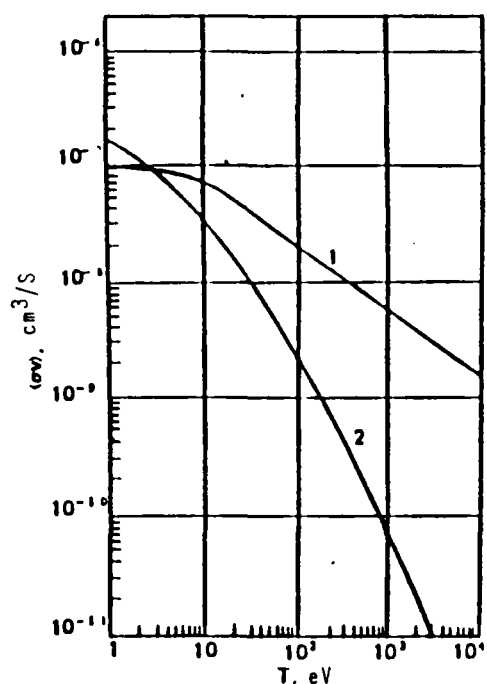
Fig. 10. Dependence of the excitation rate for the 2^1S-2^3P transition on T_e: 1-[18]; 2 - present study.
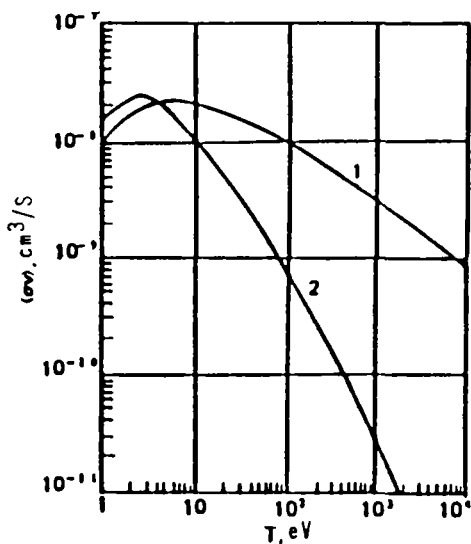
Fig. 11. Dependence of the excitation rate for the 2^3S-2^1P transition on T_e: 1-[18]; 2 - present study.
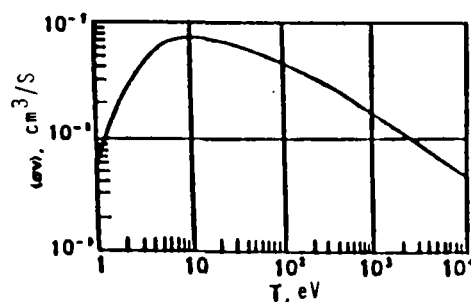
Fig. 12. Dependence of the excitation rate for the 2^3S-3^3D on T_e.
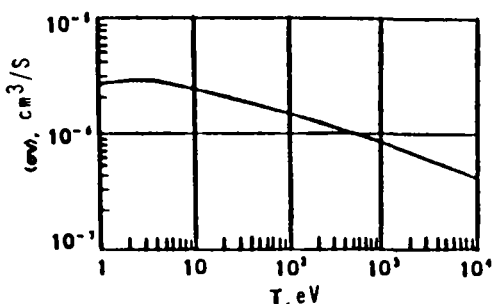
Fig. 13. Dependence of the excitation rate for the 2^1S-2^1P transition on T_e.
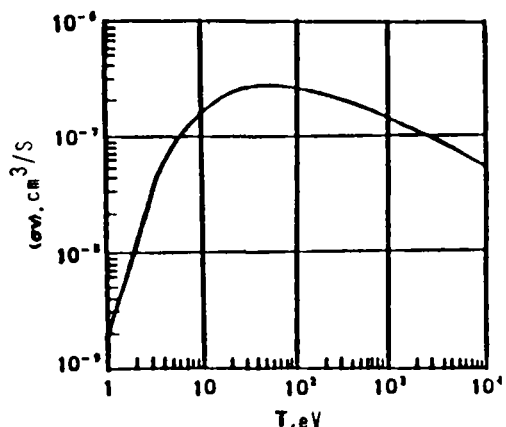
Fig. 14. Dependence of the ionization rate of the helium atom in State 2^1S on T_e.

27
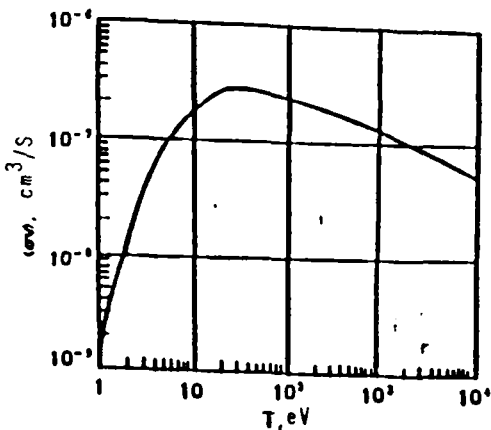
Fig. 15. Dependence of the ionization rate of the helium atom in State 2^3S on T_e.
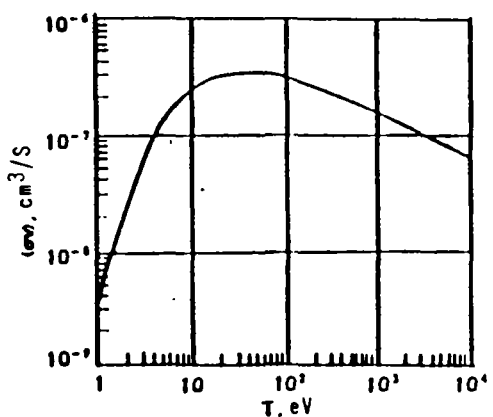
Fig. 16. Dependence of the ionization rate of the helium atom in State 2^1P on T_e.
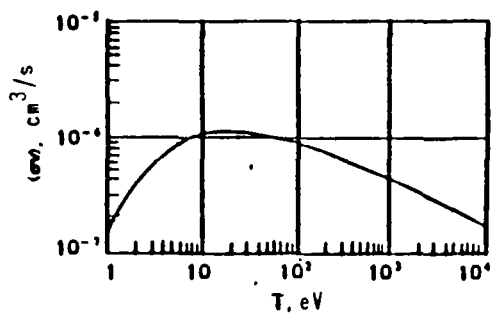
Fig. 17. Dependence of the ionization rate of helium atom in State 3^3D on T_e.
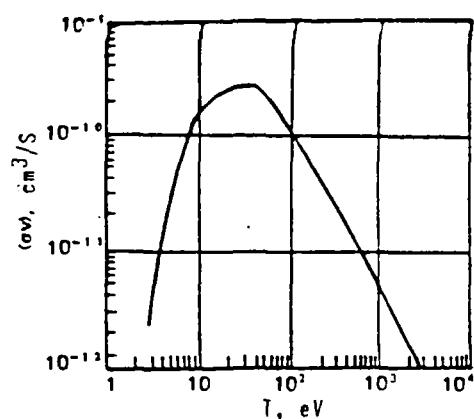
Fig. 18. Dependence of the excitation rate for the 1^1S-2^3P transition on T_e.
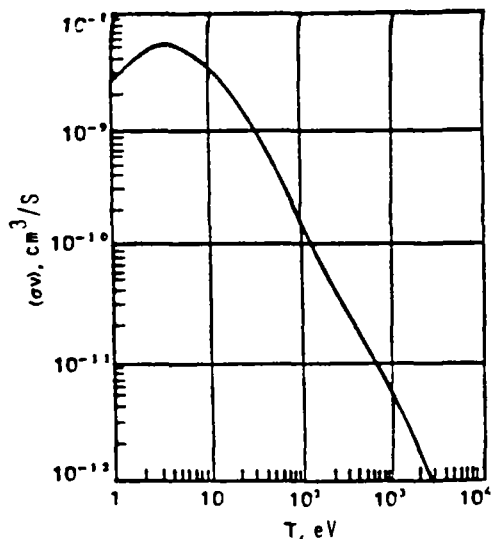
Fig. 19. Dependence of the excitation rate for the 2^1S-3^3S transition on T_e.
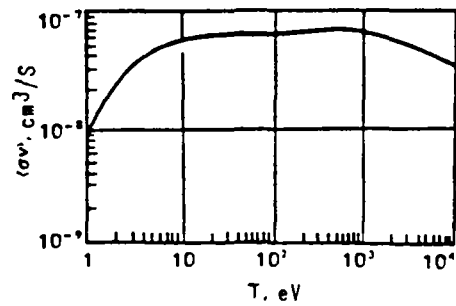
Fig. 20. Dependence of the excitation rate for 2^1S-3^1P transition on T_e.

2.4.   Ionization and recombination cross-sections

The electron-impact ionization cross-sections for the helium atom and ion from the ground state were calculated in the various approximations by a number of authors.

The results of the various studies are analysed in detail in Ref. [36], which gives the recommended values for both ionization cross-sections and ionization rates. The comparison of the results of Ref. [36] with those of calculation using the data of Ref. [22] shows that the agreement is sufficiently satisfactory. The data of Ref. [22] can be used to calculate the cross-sections for ionization from the excited states of the helium atom with $n = 2$ to 4, while for levels with $n \geq 5$ the numerous calculation results for the hydrogen atom can be employed.

The cross-sections for photorecombination into the different levels can also be found by the "Atom" program. According to Ref. [7], the rate of photorecombination $K_\nu(a)$ into a particular level $\underline{a}$ with ionization energy E_a is given by the expression:

$$K_\nu(a) = 10^{-8} (DE/R_y)^{1/2} \frac{Q_r A \beta^{3/2}}{\beta + \chi} [\frac{cm^3}{s}],$$

where $DE = |2Ry|$, $\beta = |DE|/T$.

The multiplier Q_r depends only on the angular moments of state $\underline{a}$ [22]. For the He^{++} ion $Q_r = 1$ while for the He^+ ion $Q_r = 1/2$ for recombination into the ground state $1s^2$ and $Q_r = 1$ for recombination into the excited states. The values of parameters A and χ for recombination into some states are given in Table 12. The contribution of the recombination into a level with a given S is proportional to $(2S + 1)$.

For levels with $n \geq 3$ the results obtained in the case of the hydrogen atom can be used with satisfactory accuracy.

The Burgess formula can be used to calculate the total dielectronic recombination rate of the He^+ ion. For high electron densities we should take into account the corrections obtained in a number of studies (see, for

Table 12

Constants	Level		
	1^1S_0	$2^1S + 2^3S$	$2^1P + 2^3P$
A	$2.57.10^{-4}$	$1.73.10^{-4}$	$6.7.10^{-4}$
x	0.12	$3.8.10^{-2}$	0.48

example, Ref. [37]). The contribution of the dielectronic recombination to the level population of the helium atom with a fixed value n can be evaluated with the use of the results of Ref. [22].

2.5. Probabilities of intercombination radiative transitions

For relatively low electron densities or low electron temperatures, not only the collisional processes can be substantial but also the radiative processes associated with spin-changing transitions ($\Delta S = 1$). In the case of the helium atom, the most important radiative transitions are $2^3P - 1^1S_0$, $2^3P_1 - 2^1S_0$, $2^1P_1 - 2^3S_1$, and for their probabilities the following values are given in Ref. [38]: $W(2^3P_1 - 1^1S_0) = 1.8 \times 10^2$ s^{-1}, $W(2^3P_1 - 2^1S_0) = 0.027$ s^{-1}, $W(2^1P_1 - 2^3S_1) = 1.55$ s^{-1}. In determining the the 2^3P level population it is of interest to evaluate the limiting density n_{cr}, which separates the regions where the predominant role is played by collisions and by radiative processes with change of spin (for $n_e > n_{cr}$ the principal role is played by spin-changing collisions and for $n_e < n_{cr}$ the principal role is played by spin-changing radiative processes). The values of n_{cr} for a number of values of T_e are given in Table 13.

It can be seen that in a boundary plasma with $n_e = 10^{12}$ to 10^{14} cm^{-3} and $T_e = 3$ to 100 eV, in determining the 2^3P level population, the contribution of the intercombination radiative transitions cannot be neglected in advance.

Table 13

T_e, eV	n_{cr}, cm^{-3}	T_e, eV	n_{cr}, cm^{-3}	T_e, eV	n_{cr}, cm^{-3}
3	2.10^{14}	15	7.10^{11}	70	10^{12}
4	2.10^{13}	20	6.10^{11}	100	$1,3.10^{12}$
5	10^{13}	30	6.10^{11}		
10	10^{12}	50	7.10^{11}		

3. ANALYSIS OF COLLISION CROSS-SECTION DATA FOR THE HYDROGEN ATOM

In Ref. [6] we find the semi-empirical dependences for K_{nc} - the electron ionization rate of the hydrogen atom in state n, for K_{nm} - the electron-impact excitation rate for the transition between levels with principal quantum numbers n and m and for $\alpha_{(n)}^{(2)}$ - the radiative recombination into level n. According to Ref. [6], we have:

$$K_{nc}(T_e) = 1.17935 \cdot 10^{-8} \sqrt{T_e}\ n^2 Y_n^2 \Phi_i(n, T_e)\left[\frac{cm^3}{s}\right],$$

$$\Phi_i(n, T_e) = A_n\left[E_1(Y_n)/Y_n - E_1(Z_n)/Z_n\right] + (B_n - A_n \ln 2n^2) \times$$

$$\times\ [\xi(Y_n) - \xi(Z_n)], \tag{21}$$

$$B_n = \frac{2}{3}n^2(5 + b_n);\quad A_n = \frac{32}{3\sqrt{3}}\ n \sum_{i=0}^{2} \frac{\varphi_i(n)}{i+3}, \tag{22}$$

$$Y_n = I_n/T_e;\quad Z_n = Y_n + r_n,\quad \xi(t) = E_0(t) - 2E_1(t) + E_2(t),$$

where $E_i(t) = \int_1^{\infty} e^{-xt} x^{-1} dx$ and I_n the ionization energy of level n (I_n and T_e, eV);

$$K_{nm} = 1.17935 \cdot 10^{-8} \sqrt{T_e}\ \Psi_{nm} Y_{nm} \Phi_w(n, m, T_e)\left[\frac{cm^3}{s}\right]. \tag{23}$$

$$\Phi_w(n, m, T_e) = A_{nm}\left[\left(\frac{1}{Y_{nm}} + \frac{1}{2}\right)E_1(Y_{nm}) - \left(\frac{1}{Z_{nm}} + \frac{1}{2}\right) \times\right.$$

$$\left.\times\ E_1(Z_{nm})\right] + (B_{nm} - A_{nm}\ln \Psi_{nm})[E_2(Y_{nm})/Y_{nm} - E_2(Z_{nm})/Z_{nm}].$$

$$Y_{nm} = \Delta E_{nm}/T_e;\quad Z_{nm} = Y_{nm} + r_{nm};\quad \Psi_{nm} = 2n^2 x,$$

$$r_{nm} = r_n \cdot x,\quad x = 1 - \left(\frac{n}{m}\right)^2,$$

$$B_{nm} = \Psi_{nm}^2\left(1 + \frac{4}{3x} + \frac{b_n}{x^2}\right)/m^3,\quad A_{nm} = \Psi_{nm}\ f_{absp.}^{nm}, \tag{24}$$

$$b_n = \begin{cases} -0.603, & n = 1, \\ (4 - 18.63/n + 36.24/n^2 - 28.05/n^3)/n, & n \geqslant 2, \end{cases}$$

$$r_n = \begin{cases} 0.45, & n = 1, \\ 1.94\ n^{-1.57}, & n \geqslant 2. \end{cases}$$

Here ΔE_{nm} is the transition energy, eV.

$$\alpha_n^{(2)} = 5.197 \cdot 10^{-14} \beta_n^{3/4} \exp(-\beta_n) \sum_{i=0}^{2} \varphi_i(n) E_{i+1}(\beta_n)\left[\frac{cm^3}{s}\right]. \tag{25}$$

where $\beta_n = I_n/T_e$.

Approximate formulae for the rates of the above processes are also

given in Ref. [22]:

$$K_{nc} = 10^{-8} \left(\frac{13.6}{I_n} \right)^{3/2} e^{-\beta} \left(\frac{\beta}{\beta + 1} \right)^{1/2} \frac{A_1}{\beta + \chi_1} , \qquad (26)$$

where $\beta = I_n / T_e$;

$$K_{nm} = 10^{-8} \left(\frac{13.6}{\Delta E_{nm}} \right)^{3/2} \left(\frac{E_m}{E_n} \right)^{3/2} \frac{1}{2l_0 + 1} e^{-\beta} A_2 \frac{\sqrt{\beta(\beta + 1)}}{\beta + \chi_2} , \qquad (27)$$

where E_n, E_m are the energies of levels n and m, reckoned from the

ionization limit;

$$\alpha_n^{(2)} = 10^{-13} \left(\frac{|E_n|}{13.6} \right)^{1/2} \frac{A_3 \beta_n^{3/2}}{\beta_n + \chi_3} , \qquad (28)$$

where $\beta_n = |E_n| / T_e$.

The parameters A_1, A_2, A_3, χ_1, χ_2, χ_3 for a number of levels are

given in Ref. [22]. Figures 21-26 present the results of comparison of the

ionization and excitation rates calculated in accordance with Refs [39, 6, 40]

and Ref. [22]. We note that the data of Ref. [22] agree satisfactorily with

the results of the corresponding calculations by the "Atom" program. It will

be seen that in the temperature region of interest to us the agreement between

the results of calculation by the different models is fully satisfactory.
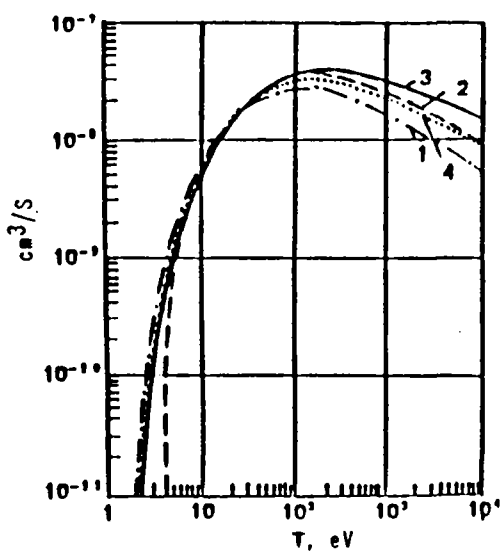
Fig. 21. Dependence of the
ionization rate of hydrogen
atom in the ground state on
T_e: 1-[39]; 2-[6]; 3-[40];
4-[36].
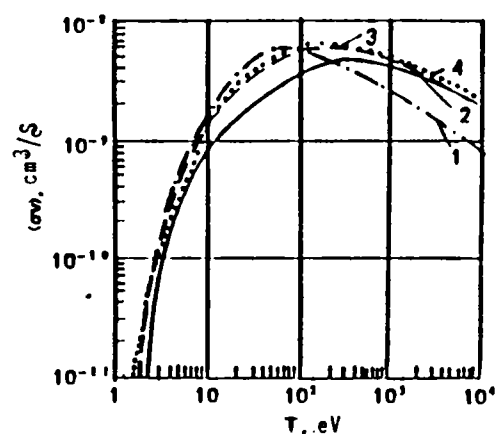
Fig. 22. Dependence of the
excitation rate for n = 1 to 3
transition in the hydrogen atom
on T_e: 1-[22]; 2-[39]; 3-[6];
4-[40].
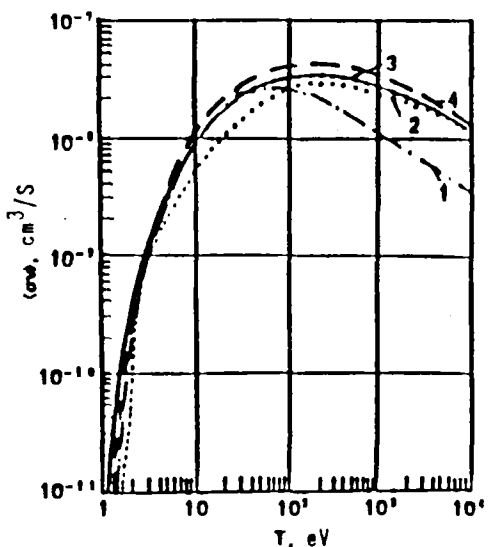
Fig. 23. Dependence of the
excitation rate for n = 1 to 2
transition in the hydrogen atom
on T_e: 1-[22]; 2-[39]; 3-[6];
4-[40].
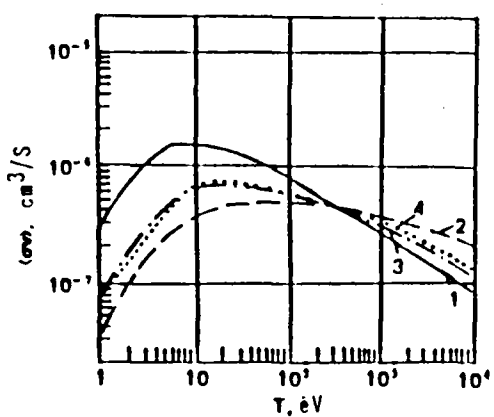
Fig. 24. Dependence of the
excitation rate for the n = 2 to 3
transition in the hydrogen atom
on T_e: 1-[22]; 2-[39]; 3-[6];
4-[40].
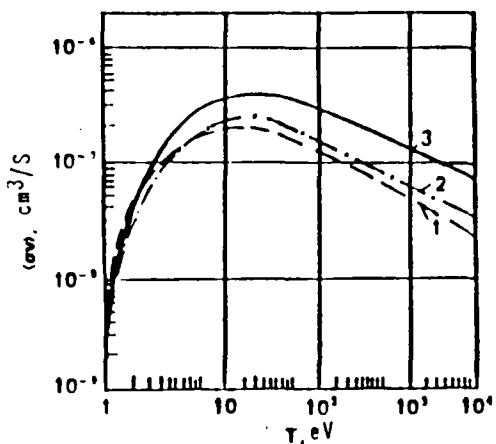
Fig. 25. Dependence of the
ionization rate of the hydrogen
atom in the state with n = 2 on T_e.
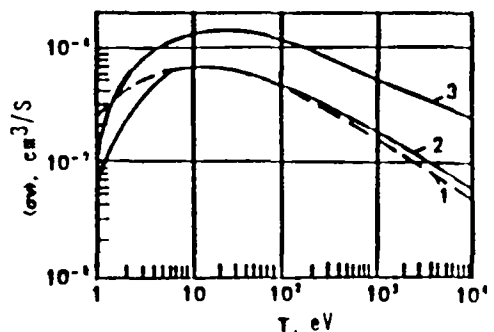
Fig. 26. Dependence of the
ionization rate of the hydrogen
atom in the state with n = 3 on T_e.

Thus, in the case of the hydrogen atom we can recommend the use of the
excitation cross-sections for the different levels and the ionization cross-
sections calculated in Ref. [22].

IV.   RESULTS OF KINETIC CALCULATIONS

Applying the kinetic model described in Section II, for calculation of
the populations of the different levels of the hydrogen and helium atoms with
the help of the data on reaction rates given in Section III, we calculated a

number of characteristics of the optically thin hydrogen and helium plasmas.

In order to determine the number of levels of the atom which are formed in the

plasma, we used the evaluations which took into account the influence of the

Lorentz ionization and the ionization in the static microfield of ions in the

plasma. For the characteristic parameters of the divertor plasma, about

25 levels are usually taken. In the calculations n_{bound} was chosen in the

form:

$$n_{rp} = \max(25, n_c^D),$$

$$n_c^D = \sqrt{5.6 \quad 10^4 Z \sqrt{T_e}/[n_e(z+1)]}.$$

(29)

Here Z is the charge; T_e in units of eV and n_e in units of 10^{13} cm^{-3}.

It is of utmost interest to find the dependence on n_e and T_e of

such characteristics as the effective ionization rate, the effective

recombination rate, the "ion cost" and the power of line radiation (both total

and for individual lines). Table 14 gives the results of calculation of the

ionization rate for the hydrogen atom in the region of $n_e = 10^{10} - 10^{16}$ cm^3

and $T_e = 1 - 10^3$ eV and Table 15 the effective recombination rates for the

hydrogen plasma. There is good agreement between the results of calculation

and those of Ref. [41], indicating the reliability of the chosen data and

calculation scheme. Table 16 presents the data for the "ion cost" in a

hydrogen plasma ("ion cost" usually means the sum of ionization potential and

energy radiated by the atom during the time up to ionization). Table 17

contains the results of calculations for the reduced line radiation intensity

of the hydrogen plasma in eV.cm^3.s^{-1}. Table 18 and 19 present the data

for the reduced

intensity of the H_α and H_β lines in eV.cm^3.s^{-1}. Table 20 shows the effective

ionization rate for the helium atom with allowance for multistep processes.

Similar calculations were performed for the helium plasma also. Table 21

gives the values of the effective rate of recombination with helium atom

formation. Table 22 gives the "ion cost" (C_{ion}) for He$^+$. Table 23

presents the values of the reduced line radiation intensity for the helium

34

Table 14 Effective ionization rate for the hydrodgen atom, cm^3/s

T_e, eV	n_e, cm^{-3}									
	1.000+10	1.000+11	1.000+12	5.000+12	1.000+13	5.000+13	1.000+14	5.000+14	1.000+15	1.000+16
1.0	0.578-14	0.698-14	0.975-14	0.142-13	0.176-13	0.346-13	0.498-13	0.140-12	0.230-12	0.795-12
2.0	0.825-11	0.918-11	0.112-10	0.141-10	0.162-10	0.250-10	0.320-10	0.669-10	0.931-10	0.172-9
3.0	0.107-9	0.116-9	0.134-9	0.160-9	0.178-9	0.250-9	0.304-9	0.551-9	0.707-9	0.106-8
4.0	0.411-9	0.438-9	0.495-9	0.573-9	0.626-9	0.835-9	0.990-9	0.165-8	0.202-8	0.277-8
5.0	0.252-9	0.101-8	0.112-8	0.127-8	0.138-8	0.178-8	0.207-8	0.325-8	0.389-8	0.505-8
6.0	0.170-8	0.178-8	0.196-8	0.221-8	0.237-8	0.300-8	0.345-8	0.522-8	0.611-8	0.769-8
7.0	0.260-8	0.272-8	0.297-8	0.331-8	0.354-8	0.440-8	0.502-8	0.740-8	0.855-8	1.151-8
8.0	0.361-8	0.376-8	0.409-8	0.452-8	0.482-8	0.592-8	0.671-8	0.968-8	1.108-8	1.341-8
9.0	0.468-8	0.487-8	0.526-8	0.580-8	0.616-8	0.750-8	0.845-8	1.199-8	1.343-8	1.531-8
10.0	0.579-8	0.601-8	0.648-8	0.710-8	0.752-8	0.909-8	1.021-8	1.429-8	1.615-8	1.716-8
20.0	1.587-8	1.635-8	1.732-8	1.854-8	1.952-8	2.279-8	2.509-8	3.313-8	3.662-8	4.205-8
30.0	2.260-8	2.320-8	2.444-8	2.612-8	2.723-8	3.141-8	3.433-8	4.452-8	4.806-8	5.593-8
40.0	2.685-8	2.753-8	2.891-8	3.078-8	3.202-8	3.667-8	3.903-8	5.135-8	5.639-8	6.435-8
50.0	2.760-8	3.031-8	3.177-8	3.373-8	3.504-8	3.996-8	4.339-8	5.553-8	6.096-8	6.367-8
60.0	3.139-8	3.213-8	3.362-8	3.564-8	3.607-8	4.203-8	4.555-8	5.811-8	6.382-8	7.308-8
70.0	3.258-8	3.332-8	3.483-8	3.687-8	3.822-8	4.334-8	4.600-8	5.979-8	6.559-8	7.529-8
80.0	3.336-8	3.410-8	3.561-8	3.766-8	3.901-8	4.414-8	4.772-8	6.063-8	6.666-8	7.569-8
90.0	3.385-8	3.460-8	3.610-8	3.814-8	3.949-8	4.461-8	4.818-8	6.113-8	6.724-8	7.155-8
100.0	3.415-8	3.489-8	3.639-8	3.841-8	3.975-8	4.484-8	4.839-8	6.133-8	6.750-8	7.303-8
200.0	3.326-8	3.393-8	3.526-8	3.706-8	3.824-8	4.278-8	4.504-8	5.789-8	6.406-8	7.552-8
300.0	3.112-8	3.172-8	3.291-8	3.452-8	3.557-8	3.962-8	4.245-8	5.330-8	5.919-8	7.182-8
400.0	2.921-8	2.975-8	3.084-8	3.231-8	3.327-8	3.694-8	3.951-8	4.949-8	5.509-8	6.568-8
500.0	2.760-8	2.811-8	2.912-8	3.047-8	3.135-8	3.474-8	3.711-8	4.638-8	5.172-8	6.320-8
600.0	2.625-8	2.673-8	2.767-8	2.893-8	2.976-8	3.291-8	3.512-8	4.381-8	4.802-8	6.027-8
700.0	2.510-8	2.555-8	2.644-8	2.763-8	2.840-8	3.137-8	3.344-8	4.165-8	4.656-8	5.777-8
800.0	2.411-8	2.453-8	2.538-8	2.650-8	2.723-8	3.004-8	3.201-8	3.979-8	4.452-8	5.559-8
900.0	2.324-8	2.364-8	2.445-8	2.552-8	2.622-8	2.888-8	3.076-8	3.818-8	4.275-8	5.368-8
1000.0	2.246-8	2.286-8	2.363-8	2.465-8	2.532-8	2.787-8	2.965-8	3.677-8	4.119-8	5.198-8

*) 0.578 − 14, means $0.578.10^{-14}$.

Table 15 Effective recombination rate in the hydrogen plasma, cm^3/s

T_e, eV	n_e, cm^{-3}									
	1.000+10	1.000+11	1.000+12	5.000+12	1.000+13	5.000+13	1.000+14	5.000+14	1.000+15	1.000+16
1	2	3	4	5	6	7	8	9	10	11
1.0	0.428-12	0.489-12	0.615-12	0.790-12	0.905-12	0.137-11	0.170-11	0.321-11	0.462-11	0.151-10
2.0	0.238-12	0.255-12	0.287-12	0.327-12	0.352-12	0.439-12	0.403-12	0.720-12	0.885-12	0.153-11
3.0	0.170-12	0.178-12	0.192-12	0.209-12	0.220-12	0.254-12	0.275-12	0.356-12	0.407-12	0.374-12
4.0	0.134-12	0.138-12	0.146-12	0.155-12	0.161-12	0.179-12	0.189-12	0.229-12	0.252-12	0.325-12
5.0	0.111-12	0.114-12	0.119-12	0.124-12	0.128-12	0.138-12	0.145-12	0.167-12	0.179-12	0.220-12
6.0	0.951-13	0.969-13	0.100-12	0.104-12	0.106-12	0.113-12	0.117-12	0.131-12	0.139-12	0.165-12
7.0	0.833-13	0.846-13	0.869-13	0.895-13	0.911-13	0.958-13	0.985-13	0.108-12	0.113-12	0.131-12
8.0	0.743-13	0.752-13	0.769-13	0.788-13	0.798-13	0.832-13	0.851-13	0.916-13	0.949-13	0.109-12
9.0	0.670-13	0.677-13	0.690-13	0.704-13	0.712-13	0.736-13	0.750-13	0.796-13	0.819-13	0.931-13
10.0	0.611-13	0.616-13	0.626-13	0.636-13	0.642-13	0.660-13	0.670-13	0.704-13	0.721-13	0.312-13
20.0	0.325-13	0.326-13	0.326-13	0.327-13	0.327-13	0.327-13	0.327-13	0.327-13	0.328-13	0.354-13
30.0	0.221-13	0.220-13	0.220-13	0.219-13	0.219-13	0.217-13	0.216-13	0.213-13	0.212-13	0.225-13
40.0	0.166-13	0.166-13	0.165-13	0.164-13	0.164-13	0.162-13	0.160-13	0.157-13	0.155-13	0.163-13
50.0	0.132-13	0.132-13	0.131-13	0.130-13	0.130-13	0.128-13	0.127-13	0.123-13	0.122-13	0.127-13
60.0	0.109-13	0.109-13	0.109-13	0.108-13	0.107-13	0.106-13	0.105-13	0.102-13	0.100-13	0.104-13
70.0	0.931-14	0.929-14	0.923-14	0.916-14	0.912-14	0.897-14	0.888-14	0.860-14	0.848-14	0.372-14
80.0	0.808-14	0.806-14	0.801-14	0.794-14	0.790-14	0.777-14	0.769-14	0.743-14	0.733-14	0.750-14
90.0	0.712-14	0.710-14	0.705-14	0.699-14	0.696-14	0.684-14	0.677-14	0.653-14	0.644-14	0.556-14
100.0	0.635-14	0.633-14	0.629-14	0.624-14	0.620-14	0.609-14	0.603-14	0.582-14	0.573-14	0.582-14
200.0	0.292-14	0.291-14	0.289-14	0.287-14	0.285-14	0.280-14	0.277-14	0.266-14	0.261-14	0.260-14
300.0	0.182-14	0.182-14	0.180-14	0.179-14	0.178-14	0.175-14	0.173-14	0.166-14	0.163-14	0.161-14
400.0	0.129-14	0.129-14	0.128-14	0.127-14	0.126-14	0.124-14	0.123-14	0.118-14	0.116-14	0.113-14
500.0	0.989-15	0.986-15	0.979-15	0.971-15	0.966-15	0.949-15	0.938-15	0.904-15	0.886-15	0.363-15
600.0	0.792-15	0.789-15	0.784-15	0.778-15	0.774-15	0.760-15	0.752-15	0.725-15	0.710-15	0.590-15
700.0	0.655-15	0.653-15	0.649-15	0.644-15	0.640-15	0.629-15	0.623-15	0.601-15	0.589-15	0.570-15
800.0	0.556-15	0.554-15	0.550-15	0.546-15	0.543-15	0.534-15	0.528-15	0.510-15	0.409-15	0.482-15
900.0	0.480-15	0.478-15	0.475-15	0.472-15	0.469-15	0.461-15	0.457-15	0.441-15	0.432-15	0.416-15
1000.0	0.421-15	0.419-15	0.417-15	0.413-15	0.411-15	0.405-15	0.400-15	0.387-15	0.379-15	0.365-15

Table 16 C_{ion} in the hydrogen plasma, eV

T_e, eV	n_e, cm^{-3}									
	1.000+1	1.000+11	1.000+12	5.000+12	1.000+13	5.000+13	1.000+14	5.000+14	1.000+15	1.000+16
1.0	2.235+ 3	1.849+ 3	1.324+ 3	9.078+ 2	7.324+ 2	3.747+ 2	2.608+ 2	9.433+ 1	5.835+ 1	1.359+ 1
2.0	2.522+ 2	2.267+ 2	1.863+ 2	1.480+ 2	1.293+ 2	8.433+ 1	6.658+ 1	3.342+ 1	2.468+ 1	1.489+ 1
3.0	1.160+ 2	1.073+ 2	9.278+ 1	7.801+ 1	7.035+ 1	5.074+ 1	4.218+ 1	2.468+ 1	1.995+ 1	1.433+ 1
4.0	7.830+ 1	7.347+ 1	6.518+ 1	5.646+ 1	5.180+ 1	3.942+ 1	3.371+ 1	2.152+ 1	1.814+ 1	1.412+ 1
5.0	6.192+ 1	5.862+ 1	5.291+ 1	4.658+ 1	4.310+ 1	3.397+ 1	2.957+ 1	1.994+ 1	1.724+ 1	1.402+ 1
6.0	5.395+ 1	5.147+ 1	4.709+ 1	4.196+ 1	3.854+ 1	3.083+ 1	2.717+ 1	1.901+ 1	1.671+ 1	1.396+ 1
7.0	4.759+ 1	4.547+ 1	4.172+ 1	3.756+ 1	3.528+ 1	2.882+ 1	2.562+ 1	1.841+ 1	1.637+ 1	1.392+ 1
8.0	4.399+ 1	4.209+ 1	3.884+ 1	3.521+ 1	3.318+ 1	2.744+ 1	2.455+ 1	1.800+ 1	1.613+ 1	1.389+ 1
9.0	4.128+ 1	3.967+ 1	3.676+ 1	3.350+ 1	3.147+ 1	2.643+ 1	2.377+ 1	1.770+ 1	1.596+ 1	1.387+ 1
10.0	3.932+ 1	3.786+ 1	3.521+ 1	3.222+ 1	3.053+ 1	2.567+ 1	2.318+ 1	1.747+ 1	1.583+ 1	1.386+ 1
20.0	3.196+ 1	3.104+ 1	2.934+ 1	2.736+ 1	2.622+ 1	2.279+ 1	2.007+ 1	1.665+ 1	1.537+ 1	1.380+ 1
30.0	3.104+ 1	2.920+ 1	2.792+ 1	2.612+ 1	2.512+ 1	2.210+ 1	2.046+ 1	1.650+ 1	1.529+ 1	1.380+ 1
40.0	2.920+ 1	2.842+ 1	2.717+ 1	2.560+ 1	2.468+ 1	2.184+ 1	2.030+ 1	1.648+ 1	1.529+ 1	1.380+ 1
50.0	2.875+ 1	2.808+ 1	2.683+ 1	2.534+ 1	2.446+ 1	2.174+ 1	2.024+ 1	1.650+ 1	1.531+ 1	1.380+ 1
60.0	2.848+ 1	2.78 + 1	2.664+ 1	2.520+ 1	2.435+ 1	2.170+ 1	2.024+ 1	1.654+ 1	1.535+ 1	1.381+ 1
70.0	2.331+ 1	2.769+ 1	2.652+ 1	2.513+ 1	2.430+ 1	2.170+ 1	2.026+ 1	1.658+ 1	1.538+ 1	1.381+ 1
80.0	2.820+ 1	2.759+ 1	2.645+ 1	2.508+ 1	2.427+ 1	2.171+ 1	2.029+ 1	1.663+ 1	1.542+ 1	1.382+ 1
90.0	2.812+ 1	2.753+ 1	2.641+ 1	2.506+ 1	2.427+ 1	2.174+ 1	2.033+ 1	1.668+ 1	1.545+ 1	1.382+ 1
100.0	2.807+ 1	2.749+ 1	2.639+ 1	2.506+ 1	2.427+ 1	2.177+ 1	2.038+ 1	1.673+ 1	1.549+ 1	1.383+ 1
200.0	2.304+ 1	2.750+ 1	2.648+ 1	2.525+ 1	2.452+ 1	2.215+ 1	2.080+ 1	1.714+ 1	1.579+ 1	1.388+ 1
300.0	2.810+ 1	2.767+ 1	2.669+ 1	2.550+ 1	2.478+ 1	2.247+ 1	2.114+ 1	1.745+ 1	1.602+ 1	1.391+ 1
400.0	2.835+ 1	2.784+ 1	2.688+ 1	2.571+ 1	2.501+ 1	2.272+ 1	2.141+ 1	1.770+ 1	1.621+ 1	1.395+ 1
500.0	2.850+ 1	2.799+ 1	2.704+ 1	2.589+ 1	2.520+ 1	2.294+ 1	2.164+ 1	1.790+ 1	1.638+ 1	1.397+ 1
600.0	2.863+ 1	2.813+ 1	2.719+ 1	2.605+ 1	2.537+ 1	2.312+ 1	2.183+ 1	1.808+ 1	1.652+ 1	1.400+ 1
700.0	2.875+ 1	2.825+ 1	2.732+ 1	2.619+ 1	2.551+ 1	2.328+ 1	2.199+ 1	1.824+ 1	1.664+ 1	1.402+ 1
800.0	2.886+ 1	2.836+ 1	2.744+ 1	2.631+ 1	2.564+ 1	2.343+ 1	2.214+ 1	1.838+ 1	1.675+ 1	1.404+ 1
900.0	2.895+ 1	2.846+ 1	2.754+ 1	2.643+ 1	2.576+ 1	2.355+ 1	2.227+ 1	1.850+ 1	1.686+ 1	1.406+ 1
1000.0	2.904+ 1	2.855+ 1	2.764+ 1	2.653+ 1	2.586+ 1	2.367+ 1	2.239+ 1	1.862+ 1	1.695+ 1	1.408+ 1

Table 17   Reduced power of line radiation of the hydrogen plasma,
eV.cm^3.s^1

T_e, eV	$1.000+11$	$5.000+11$	$1.000+12$	$5.000+12$	$1.000+13$	$5.000+13$	$1.000+14$	$5.000+14$	$1.000+15$	$1.000+16$
1.0	0.128-10	0.125-10	0.128-10	0.127-10	0.127-10	0.125-10	0.123-10	0.113-10	0.103-10	0.500-11
2.0	0.197-8	0.196-8	0.193-8	0.189-8	0.187-8	0.177-8	0.169-8	0.133-8	0.105-8	0.223-9
3.0	1.078-8	1.056-8	1.043-8	1.031-8	1.010-8	0.929-8	0.870-8	0.611-8	0.449-8	0.781-9
4.0	2.640-8	2.624-8	2.552-8	2.456-8	2.303-8	2.157-8	1.991-8	1.305-8	0.919-8	0.146-8
5.0	4.578-8	4.527-8	4.393-8	4.195-8	4.072-8	3.621-8	3.307-8	2.068-8	1.418-8	0.213-8
6.0	6.698-8	6.554-8	6.356-8	6.058-8	5.865-8	5.163-8	4.680-8	2.830-8	1.907-8	0.278-8
7.0	9.832-8	8.672-8	8.353-8	7.938-8	7.660-8	6.702-8	6.038-8	3.564-8	2.372-8	0.339-8
8.0	1.093-7	1.072-7	1.031-7	9.776-8	9.431-8	8.194-8	7.350-8	4.260-8	2.811-8	0.395-8
9.0	1.295-7	1.270-7	1.220-7	1.154-7	1.112-7	9.622-8	8.601-8	4.917-8	3.223-8	0.448-8
10.0	1.499-7	1.459-7	1.400-7	1.323-7	1.274-7	1.098-7	9.786-8	5.535-8	3.610-8	0.498-8
20.0	2.916-7	2.852-7	2.728-7	2.556-7	2.443-7	2.096-7	1.851-7	1.012-7	6.499-8	0.376-8
30.0	3.716-7	3.636-7	3.477-7	3.271-7	3.139-7	2.671-7	2.358-7	1.293-7	8.316-8	1.123-8
40.0	4.191-7	4.191-7	3.924-7	3.695-7	3.549-7	3.024-7	2.676-7	1.480-7	9.568-8	1.502-8
50.0	4.295-7	4.391-7	4.235-7	3.963-7	3.898-7	3.253-7	2.885-7	1.613-7	1.048-7	1.438-8
60.0	4.676-7	4.577-7	4.385-7	4.137-7	3.978-7	3.407-7	3.027-7	1.710-7	1.117-7	1.546-8
70.0	4.705-7	4.696-7	4.503-7	4.251-7	4.000-7	3.511-7	3.127-7	1.784-7	1.171-7	1.634-8
80.0	4.372-7	4.773-7	4.578-7	4.326-7	4.165-7	3.583-7	3.197-7	1.841-7	1.214-7	1.707-8
90.0	4.218-7	4.823-7	4.626-7	4.374-7	4.214-7	3.633-7	3.247-7	1.885-7	1.248-7	1.769-8
100.0	4.345-7	4.847-7	4.654-7	4.404-7	4.244-7	3.666-7	3.282-7	1.921-7	1.277-7	1.323-8
200.0	4.805-7	4.717-7	4.544-7	4.320-7	4.178-7	3.658-7	3.312-7	2.051-7	1.407-7	2.125-8
300.0	4.543-7	4.464-7	4.309-7	4.108-7	3.933-7	3.514-7	3.204-7	2.054-7	1.438-7	2.263-8
400.0	4.311-7	4.233-7	4.097-7	3.814-7	3.707-7	3.372-7	3.089-7	2.030-7	1.443-7	2.345-8
500.0	4.114-7	4.047-7	3.915-7	3.747-7	3.630-7	3.246-7	2.984-7	1.998-7	1.438-7	2.400-8
600.0	3.743-7	3.882-7	3.762-7	3.603-7	3.503-7	3.136-7	2.891-7	1.965-7	1.429-7	2.441-8
700.0	3.304-7	3.744-7	3.629-7	3.479-7	3.385-7	3.039-7	2.808-7	1.933-7	1.418-7	2.471-8
800.0	3.679-7	3.622-7	3.512-7	3.371-7	3.281-7	2.953-7	2.734-7	1.902-7	1.406-7	2.496-8
900.0	3.568-7	3.514-7	3.409-7	3.274-7	3.189-7	2.877-7	2.668-7	1.873-7	1.394-7	2.516-8
1000.0	3.470-7	3.413-7	3.317-7	3.193-7	3.106-7	2.808-7	2.607-7	1.846-7	1.382-7	2.532-8

Table 18   Reduced power of H_α line radiation, $eV.cm^3.s^{-1}$

T_e, eV	n_e, cm^{-3}									
	1.000+10	5.000+11	1.000+12	5.000+12	1.000+13	5.000+13	1.000+14	5.000+14	1.000+15	1.000+16
1	2	3	4	5	6	7	8	9	10	11
1.0	0.319−13	0.310−13	0.309−13	0.290−13	0.280−13	0.217−13	0.184−13	0.124−13	0.106−13	0.379−14
2.0	0.123−10	0.120−10	0.115−10	0.104−10	0.937−11	0.593−11	0.454−11	0.243−11	0.178−11	0.548−12
3.0	0.914−10	0.895−10	0.844−10	0.735−10	0.647−10	0.376−10	0.277−10	0.133−10	0.910−11	0.146−11
4.0	0.254− 9	0.248− 9	0.232− 9	0.199− 9	0.172− 9	0.957−10	0.694−10	0.313−10	0.206−10	0.303−11
5.0	0.475− 9	0.463− 9	0.431− 9	0.365− 9	0.314− 9	0.170− 9	0.122− 9	0.529−10	0.339−10	0.476−11
6.0	0.728− 9	0.709− 9	0.658− 9	0.553− 9	0.472− 9	0.252− 9	0.179− 9	0.758−10	0.478−10	0.552−11
7.0	0.904− 9	0.967− 9	0.876− 9	0.749− 9	0.638− 9	0.336− 9	0.238− 9	0.989−10	0.617−10	0.326−11
8.0	0.126− 8	0.123− 8	0.113− 8	0.966− 9	0.803− 9	0.421− 9	0.297− 9	0.122− 9	0.753−10	0.994−11
9.0	0.152− 8	0.148− 8	0.137− 8	0.114− 8	0.965− 9	0.503− 9	0.355− 9	0.144− 9	0.885−10	0.116−10
10.0	0.178− 8	0.173− 8	0.159− 8	0.132− 8	0.112− 8	0.583− 9	0.411− 9	0.165− 9	0.101− 9	0.131−10
20.0	0.368− 8	0.358− 8	0.331− 8	0.275− 8	0.234− 8	0.122− 8	0.857− 9	0.336− 9	0.203− 9	0.257−10
30.0	0.476− 8	0.463− 8	0.429− 8	0.360− 8	0.308− 8	0.163− 8	0.115− 8	0.451− 9	0.273− 9	0.346−10
40.0	0.539− 8	0.525− 8	0.487− 8	0.412− 8	0.354− 8	0.191− 8	0.135− 8	0.532− 9	0.323− 9	0.413−10
50.0	0.578− 8	0.563− 8	0.524− 8	0.446− 8	0.386− 8	0.211− 8	0.149− 8	0.593− 9	0.362− 9	0.465−10
60.0	0.603− 8	0.588− 8	0.548− 8	0.468− 8	0.407− 8	0.225− 8	0.160− 8	0.640− 9	0.392− 9	0.507−10
70.0	0.619− 8	0.603− 8	0.563− 8	0.484− 8	0.422− 8	0.236− 8	0.168− 8	0.678− 9	0.416− 9	0.542−10
80.0	0.628− 8	0.613− 8	0.573− 8	0.494− 8	0.433− 8	0.244− 8	0.175− 8	0.708− 9	0.436− 9	0.572−10
90.0	0.634− 8	0.618− 8	0.579− 8	0.501− 8	0.440− 8	0.251− 8	0.180− 8	0.732− 9	0.452− 9	0.597−10
100.0	0.637− 8	0.622− 8	0.583− 8	0.506− 8	0.446− 8	0.256− 8	0.184− 8	0.753− 9	0.467− 9	0.620−10
200.0	0.616− 8	0.602− 8	0.568− 8	0.504− 8	0.452− 8	0.275− 8	0.201− 8	0.853− 9	0.540− 9	0.751−10
300.0	0.580− 8	0.567− 8	0.538− 8	0.483− 8	0.438− 8	0.275− 8	0.204− 8	0.883− 9	0.568− 9	0.815−10
400.0	0.548− 8	0.537− 8	0.511− 8	0.462− 8	0.421− 8	0.272− 8	0.203− 8	0.894− 9	0.580− 9	0.855−10
500.0	0.522− 8	0.512− 8	0.488− 8	0.443− 8	0.407− 8	0.267− 8	0.201− 8	0.897− 9	0.587− 9	0.883−10
600.0	0.500− 8	0.490− 8	0.468− 8	0.427− 8	0.393− 8	0.263− 8	0.199− 8	0.896− 9	0.590− 9	0.904−10
700.0	0.481− 8	0.472− 8	0.451− 8	0.413− 8	0.382− 8	0.258− 8	0.196− 8	0.893− 9	0.592− 9	0.921−10
800.0	0.464− 8	0.456− 8	0.436− 8	0.400− 8	0.371− 8	0.254− 8	0.194− 8	0.889− 9	0.592− 9	0.934−10
900.0	0.450− 8	0.442− 8	0.423− 8	0.389− 8	0.362− 8	0.250− 8	0.192− 8	0.884− 9	0.591− 9	0.945−10
1000.0	0.437− 8	0.429− 8	0.411− 8	0.379− 8	0.353− 8	0.246− 8	0.190− 8	0.880− 9	0.500− 9	0.955−10

Table 19 Reduced power of H_β line radiation, $eV.cm^{-3}.s^{-1}$

T_e, eV	n_e, cm^{-3}									
	1.000+10	1.000+11	1.000+12	5.000+12	1.000+13	5.000+13	1.000+14	5.000+14	1.000+15	1.000+16
1.0	0.540-14	0.521-14	0.444-14	0.301-14	0.236-14	0.130-14	0.101-14	0.630-15	0.527-15	0.186-15
2.0	0.247-11	0.271-11	0.211-11	0.125-11	0.921-12	0.425-12	0.303-12	0.146-12	0.107-12	0.207-13
3.0	0.237-10	0.222-10	0.166-10	0.932-11	0.671-11	0.290-11	0.200-11	0.887-12	0.506-12	0.945-13
4.0	0.693-10	0.647-10	0.474-10	0.259-10	0.184-10	0.770-11	0.524-11	0.219-11	0.141-11	0.205-12
5.0	0.134-9	0.124-9	0.901-10	0.485-10	0.344-10	0.141-10	0.949-11	0.382-11	0.241-11	0.334-12
6.0	0.200-9	0.194-9	0.140-9	0.747-10	0.527-10	0.213-10	0.143-10	0.560-11	0.348-11	0.468-12
7.0	0.259-9	0.269-9	0.193-9	0.103-9	0.722-10	0.290-10	0.194-10	0.745-11	0.458-11	0.504-12
8.0	0.371-9	0.345-9	0.247-9	0.131-9	0.921-10	0.368-10	0.245-10	0.930-11	0.568-11	0.739-12
9.0	0.452-9	0.419-9	0.300-9	0.159-9	0.112-9	0.446-10	0.296-10	0.111-10	0.676-11	0.370-12
10.0	0.531-9	0.492-9	0.352-9	0.187-9	0.131-9	0.525-10	0.347-10	0.129-10	0.781-11	0.998-12
20.0	0.113-8	0.105-8	0.766-9	0.414-9	0.292-9	0.116-9	0.767-10	0.278-10	0.166-10	0.207-11
30.0	0.147-8	0.137-8	0.102-8	0.562-9	0.398-9	0.160-9	0.104-9	0.383-10	0.229-10	0.286-11
40.0	0.168-8	0.157-8	0.118-8	0.662-9	0.471-9	0.191-9	0.126-9	0.460-10	0.275-10	0.346-11
50.0	0.180-8	0.169-8	0.129-8	0.732-9	0.524-9	0.214-9	0.142-9	0.519-10	0.311-10	0.394-11
60.0	0.188-8	0.177-8	0.136-8	0.783-9	0.563-9	0.232-9	0.154-9	0.565-10	0.340-10	0.433-11
70.0	0.193-8	0.181-8	0.141-8	0.822-9	0.592-9	0.245-9	0.163-9	0.602-10	0.363-10	0.466-11
80.0	0.196-8	0.185-8	0.144-8	0.851-9	0.615-9	0.256-9	0.171-9	0.632-10	0.383-10	0.493-11
90.0	0.198-8	0.187-8	0.147-8	0.874-9	0.634-9	0.263-9	0.177-9	0.658-10	0.399-10	0.518-11
100.0	0.199-8	0.188-8	0.149-8	0.892-9	0.648-9	0.273-9	0.182-9	0.679-10	0.413-10	0.539-11
200.0	0.192-8	0.183-8	0.150-8	0.953-9	0.706-9	0.307-9	0.206-9	0.790-10	0.490-10	0.566-11
300.0	0.181-8	0.173-8	0.145-8	0.950-9	0.713-9	0.316-9	0.214-9	0.830-10	0.522-10	0.731-11
400.0	0.171-8	0.164-8	0.139-8	0.934-9	0.708-9	0.318-9	0.216-9	0.849-10	0.538-10	0.772-11
500.0	0.163-8	0.156-8	0.134-8	0.916-9	0.700-9	0.318-9	0.217-9	0.858-10	0.548-10	0.801-11
600.0	0.156-8	0.150-8	0.129-8	0.898-9	0.690-9	0.317-9	0.217-9	0.862-10	0.554-10	0.823-11
700.0	0.150-8	0.144-8	0.125-8	0.881-9	0.681-9	0.315-9	0.216-9	0.864-10	0.557-10	0.841-11
800.0	0.145-8	0.139-8	0.121-8	0.865-9	0.672-9	0.314-9	0.216-9	0.864-10	0.560-10	0.856-11
900.0	0.140-8	0.135-8	0.118-8	0.850-9	0.663-9	0.312-9	0.215-9	0.863-10	0.561-10	0.868-11
1000.0	0.136-8	0.131-8	0.115-8	0.836-9	0.655-9	0.309-9	0.214-9	0.862-10	0.562-10	0.878-11

Table 20 Ionization rate for the helium atom, cm^3/s

T_e, eV	n_e, cm^{-3}
	1.000+10	1.000+11	1.000+12	5.000+12	1.000+13	5.000+13	1.000+14	5.000+14	1.000+15	1.000+16
1.0	0.300-18	0.350-18	0.696-18	0.167-17	0.246-17	0.399-17	0.446-17	0.539-17	0.630-17	0.104-16
2.0	0.636-13	0.496-13	0.998-13	0.134-12	0.154-12	0.191-12	0.225-12	0.249-12	0.279-12	0.386-12
3.0	0.336-11	0.346-11	0.396-11	0.501-11	0.551-11	0.658-11	0.707-11	0.864-11	0.967-11	0.130-10
4.0	0.250-10	0.264-10	0.289-10	0.338-10	0.362-10	0.421-10	0.451-10	0.543-10	0.606-10	0.790-10
5.0	0.889-10	0.004-10	0.966-10	0.108-9	0.114-9	0.131-9	0.140-9	0.168-9	0.185-9	0.237-9
6.0	0.204-9	0.207-9	0.216-9	0.239-9	0.250-9	0.284-9	0.301-9	0.358-9	0.394-9	0.499-9
7.0	0.373-9	0.378-9	0.395-9	0.426-9	0.444-9	0.498-9	0.528-9	0.624-9	0.684-9	0.856-9
8.0	0.591-9	0.598-9	0.621-9	0.663-9	0.688-9	0.767-9	0.810-9	0.951-9	0.104-8	0.129-8
9.0	0.850-9	0.859-9	0.888-9	0.941-9	0.974-9	0.108-8	0.114-8	0.133-8	0.143-8	0.178-8
10.0	0.114-8	0.115-8	0.119-8	0.125-8	0.129-8	0.142-8	0.150-8	0.174-8	0.189-8	0.232-8
20.0	0.476-8	0.479-8	0.484-8	0.503-8	0.513-8	0.551-8	0.573-8	0.647-8	0.672-8	0.821-8
30.0	0.827-8	0.832-8	0.843-8	0.864-8	0.879-8	0.933-8	0.965-8	1.074-8	1.142-8	1.335-8
40.0	1.121-8	1.127-8	1.141-8	1.165-8	1.183-8	1.248-8	1.288-8	1.423-8	1.507-8	1.747-8
50.0	1.361-8	1.368-8	1.383-8	1.410-8	1.429-8	1.502-8	1.548-8	1.702-8	1.799-8	2.077-8
60.0	1.558-8	1.565-8	1.581-8	1.609-8	1.630-8	1.710-8	1.760-8	1.930-8	2.036-8	2.344-8
70.0	1.724-8	1.731-8	1.748-8	1.778-8	1.800-8	1.885-8	1.938-8	2.121-8	2.235-8	2.549-8
80.0	1.861-8	1.869-8	1.884-8	1.917-8	1.940-8	2.029-8	2.085-8	2.279-8	2.400-8	2.756-8
90.0	1.975-8	1.983-8	2.001-8	2.032-8	2.057-8	2.149-8	2.208-8	2.410-8	2.537-8	2.913-8
100.0	2.070-8	2.078-8	2.096-8	2.129-8	2.153-8	2.248-8	2.309-8	2.519-8	2.652-8	3.045-8
200.0	2.508-8	2.516-8	2.535-8	2.569-8	2.596-8	2.705-8	2.776-8	3.027-8	3.187-8	3.684-8
300.0	2.588-8	2.597-8	2.616-8	2.649-8	2.676-8	2.786-8	2.861-8	3.123-8	3.291-8	3.835-8
400.0	2.592-8	2.601-8	2.619-8	2.651-8	2.677-8	2.789-8	2.859-8	3.122-8	3.292-8	3.840-8
500.0	2.575-8	2.584-8	2.601-8	2.631-8	2.656-8	2.761-8	2.833-8	3.092-8	3.260-8	3.839-8
600.0	2.541-8	2.549-8	2.566-8	2.594-8	2.617-8	2.718-8	2.789-8	3.042-8	3.207-8	3.790-8
700.0	2.500-8	2.508-8	2.524-8	2.551-8	2.573-8	2.670-8	2.739-8	2.985-8	3.146-8	3.729-8
800.0	2.455-8	2.462-8	2.479-8	2.504-8	2.525-8	2.619-8	2.685-8	2.924-8	3.081-8	3.640-8
900.0	2.408-8	2.416-8	2.431-8	2.455-8	2.476-8	2.566-8	2.630-8	2.862-8	3.015-8	3.589-8
1000.0	2.363-8	2.370-8	2.384-8	2.408-8	2.427-8	2.514-8	2.576-8	2.801-8	2.950-8	3.518-8

Table 21 Effective rate of recombination with helium atom formation, cm3/s

T_e, eV	n_e, cm^{-3}									
	1.000+10	1.000+11	1.000+12	5.000+12	1.000+13	5.000+13	1.000+14	5.000+14	1.000+15	1.000+16
1	2	3	4	5	6	7	8	9	10	11
1.0	0.513-12	0.474-12	0.952-12	0.122-11	0.138-11	0.207-11	0.262-11	0.538-11	0.790-11	0.218-10
2.0	0.231-12	0.271-12	0.321-12	0.344-12	0.359-12	0.454-12	0.524-12	0.820-12	0.105-11	0.191-11
3.0	0.148-12	0.165-12	0.184-12	0.191-12	0.178-12	0.237-12	0.264-12	0.370-12	0.444-12	0.696-12
4.0	0.123-12	0.126-12	0.133-12	0.136-12	0.140-12	0.162-12	0.176-12	0.231-12	0.268-12	0.387-12
5.0	0.146-12	0.122-12	0.114-12	0.113-12	0.114-12	0.124-12	0.135-12	0.168-12	0.190-12	0.259-12
6.0	0.228-12	0.147-12	0.114-12	0.104-12	0.103-12	0.109-12	0.114-12	0.135-12	0.149-12	0.193-12
7.0	0.363-12	0.196-12	0.126-12	0.105-12	0.100-12	0.992-13	0.102-12	0.115-12	0.124-12	0.153-12
8.0	0.540-12	0.260-12	0.144-12	0.110-12	0.102-12	0.944-13	0.947-13	0.102-12	0.107-12	0.127-12
9.0	0.740-12	0.333-12	0.166-12	0.117-12	0.105-12	0.925-13	0.906-13	0.926-13	0.961-13	0.108-12
10.0	0.949-12	0.408-12	0.189-12	0.125-12	0.110-12	0.917-13	0.880-13	0.862-13	0.877-13	0.948-13
20.0	0.234-11	0.486-12	0.323-12	0.173-12	0.137-12	0.887-13	0.762-13	0.584-13	0.534-13	0.439-13
30.0	0.434-11	0.640-12	0.327-12	0.165-12	0.128-12	0.770-13	0.638-13	0.448-13	0.305-13	0.291-13
40.0	0.237-11	0.868-12	0.294-12	0.146-12	0.112-12	0.652-13	0.531-13	0.358-13	0.310-13	0.217-13
50.0	0.213-11	0.777-12	0.261-12	0.128-12	0.970-13	0.554-13	0.447-13	0.294-13	0.253-13	0.172-13
60.0	0.190-11	0.490-12	0.231-12	0.112-12	0.844-13	0.476-13	0.392-13	0.248-13	0.211-13	0.141-13
70.0	0.160-11	0.415-12	0.205-12	0.983-13	0.742-13	0.414-13	0.331-13	0.212-13	0.191-13	0.119-13
80.0	0.151-11	0.551-12	0.183-12	0.874-13	0.657-13	0.365-13	0.290-13	0.185-13	0.157-13	0.103-13
90.0	0.136-11	0.496-12	0.165-12	0.783-13	0.588-13	0.324-13	0.257-13	0.163-13	0.138-13	0.900-14
100.0	0.124-11	0.450-12	0.149-12	0.706-13	0.529-13	0.291-13	0.230-13	0.145-13	0.123-13	0.797-14
200.0	0.596-12	0.217-12	0.718-13	0.334-13	0.248-13	0.133-13	0.105-13	0.642-14	0.538-14	0.342-14
300.0	0.370-12	0.136-12	0.449-13	0.207-13	0.153-13	0.813-14	0.635-14	0.385-14	0.322-14	0.203-14
400.0	0.261-12	0.957-13	0.318-13	0.146-13	0.107-13	0.566-14	0.441-14	0.266-14	0.221-14	0.138-14
500.0	0.197-12	0.726-13	0.242-13	0.110-13	0.811-14	0.424-14	0.331-14	0.198-14	0.165-14	0.102-14
600.0	0.157-12	0.578-13	0.193-13	0.878-14	0.643-14	0.336-14	0.261-14	0.156-14	0.129-14	0.795-15
700.0	0.129-12	0.476-13	0.159-13	0.722-14	0.528-14	0.275-14	0.213-14	0.127-14	0.105-14	0.643-15
800.0	0.109-12	0.402-13	0.135-13	0.610-14	0.445-14	0.231-14	0.179-14	0.106-14	0.877-15	0.534-15
900.0	0.933-13	0.346-13	0.116-13	0.525-14	0.382-14	0.198-14	0.153-14	0.904-15	0.748-15	0.454-15
1000.0	0.814-13	0.303-13	0.152-13	0.458-14	0.334-14	0.172-14	0.133-14	0.784-15	0.648-15	0.302-15

Table 22 C_{ion} of He+ in the helium plasma, eV

T_e, eV	n_e, cm^{-3}
	1.000+10	1.000+11	1.000+12	5.000+12	1.000+13	5.000+13	1.000+14	5.000+14	1.000+15	1.000+16
1.0	1.466+3	1.283+3	6.46?+2	2.870+2	1.2?1+2	7.2?2+1	6.392+1	5.080+1	4.477+1	2.870+1
2.0	2.383+2	1.880+2	1.344+2	7.984+1	6.6?1+1	5.103+1	4.736+1	3.936+1	3.544+1	2.652+1
3.0	1.191+2	1.151+2	9.538+1	6.958+1	6.033+1	4.9?3+1	4.557+1	3.769+1	3.398+1	2.617+1
4.0	8.890+1	8.459+1	7.597+1	6.354+1	5.513+1	4.638+1	4.335+1	3.622+1	3.290+1	2.597+1
5.0	7.497+1	7.332+1	6.620+1	5.594+1	5.192+1	4.461+1	4.186+1	3.529+1	3.222+1	2.585+1
6.0	6.695+1	6.566+1	6.056+1	5.287+1	4.966+1	4.329+1	4.076+1	3.463+1	3.175+1	2.578+1
7.0	6.169+1	6.061+1	5.664+1	5.056+1	4.787+1	4.22?+1	3.986+1	3.411+1	3.139+1	2.572+1
8.0	5.796+1	5.704+1	5.38?+1	4.878+1	4.647+1	4.133+1	3.914+1	3.369+1	3.111+1	2.548+1
9.0	5.516+1	5.436+1	5.163+1	4.736+1	4.531+1	4.060+1	3.853+1	3.335+1	3.087+1	2.544+1
10.0	5.297+1	5.226+1	4.991+1	4.618+1	4.435+1	3.998+1	3.802+1	3.306+1	3.067+1	2.542+1
20.0	4.340+1	4.303+1	4.199+1	4.028+1	3.930+1	3.656+1	3.519+1	3.148+1	2.961+1	2.546+1
30.0	4.023+1	3.992+1	3.918+1	3.799+1	3.727+1	3.512+1	3.398+1	3.079+1	2.915+1	2.540+1
40.0	3.866+1	3.839+1	3.779+1	3.683+1	3.623+1	3.434+1	3.334+1	3.043+1	2.891+1	2.537+1
50.0	3.775+1	3.751+1	3.699+1	3.617+1	3.564+1	3.392+1	3.298+1	3.023+1	2.877+1	2.535+1
60.0	3.717+1	3.696+1	3.650+1	3.576+1	3.527+1	3.364+1	3.276+1	3.011+1	2.870+1	2.534+1
70.0	3.681+1	3.660+1	3.616+1	3.548+1	3.502+1	3.348+1	3.261+1	3.003+1	2.865+1	2.534+1
80.0	3.656+1	3.636+1	3.595+1	3.530+1	3.486+1	3.337+1	3.252+1	2.999+1	2.863+1	2.534+1
90.0	3.630+1	3.620+1	3.580+1	3.519+1	3.476+1	3.331+1	3.247+1	2.997+1	2.862+1	2.534+1
100.0	3.628+1	3.610+1	3.571+1	3.512+1	3.471+1	3.329+1	3.245+1	2.997+1	2.863+1	2.534+1
200.0	3.628+1	3.612+1	3.579+1	3.528+1	3.491+1	3.356+1	3.274+1	3.025+1	2.888+1	2.542+1
300.0	3.668+1	3.652+1	3.626+1	3.572+1	3.536+1	3.401+1	3.317+1	3.061+1	2.919+1	2.550+1
400.0	3.696+1	3.679+1	3.648+1	3.601+1	3.566+1	3.432+1	3.348+1	3.088+1	2.944+1	2.557+1
500.0	3.708+1	3.693+1	3.662+1	3.618+1	3.584+1	3.452+1	3.369+1	3.108+1	2.963+1	2.564+1
600.0	3.718+1	3.703+1	3.673+1	3.630+1	3.598+1	3.468+1	3.385+1	3.125+1	2.979+1	2.569+1
700.0	3.726+1	3.711+1	3.681+1	3.640+1	3.608+1	3.480+1	3.398+1	3.139+1	2.992+1	2.574+1
800.0	3.732+1	3.717+1	3.688+1	3.647+1	3.616+1	3.491+1	3.409+1	3.151+1	3.005+1	2.579+1
900.0	3.736+1	3.722+1	3.693+1	3.653+1	3.623+1	3.499+1	3.419+1	3.161+1	3.016+1	2.583+1
1000.0	3.740+1	3.725+1	3.697+1	3.658+1	3.628+1	3.507+1	3.427+1	3.171+1	3.025+1	2.588+1

Table 23   Reduced power of line radiation of the helium plasma, eV.cm^3.s^{-1}

T_e,eV	n_e, cm^{-3} 1.000+10	1.000+11	1.000+12	5.000+12	1.000+13	5.000+13	1.000+14	5.000+14	1.000+15	1.000+16
1.0	0.445-15	0.440-15	0.431-15	0.355-15	0.257-15	0.189-15	0.175-15	0.166-15	0.129-15	0.427-16
2.0	0.117-10	0.114-10	0.997-11	0.740-11	0.640-11	0.504-11	0.468-11	0.368-11	0.303-11	0.746-12
3.0	0.318-9	0.313-9	0.283-9	0.220-9	0.197-9	0.161-9	0.148-9	0.113-9	0.909-10	0.205-10
4.0	0.167-8	0.164-8	0.148-8	0.121-8	0.111-8	0.918-9	0.845-9	0.634-9	0.503-9	0.109-9
5.0	0.448-8	0.440-8	0.403-8	0.349-8	0.313-8	0.262-8	0.241-8	0.179-8	0.141-8	0.301-9
6.0	0.864-8	0.850-8	0.735-8	0.676-8	0.628-8	0.539-8	0.497-8	0.360-8	0.283-8	0.595-9
7.0	1.385-8	1.362-8	1.266-8	1.107-8	1.034-8	0.878-8	0.807-8	0.594-8	0.465-8	0.974-9
8.0	1.973-8	1.941-8	1.815-8	1.605-8	1.506-8	1.283-8	1.179-8	0.866-8	0.678-8	0.141-8
9.0	2.598-8	2.558-8	2.492-8	2.143-8	2.019-8	1.727-8	1.586-8	1.164-8	0.909-8	0.189-8
10.0	3.246-8	3.191-8	3.009-8	2.705-8	2.555-8	2.192-8	2.014-8	1.476-8	1.152-8	0.239-8
20.0	9.960-8	9.838-8	9.485-8	7.893-8	7.598-8	6.598-8	6.079-8	4.456-8	3.478-8	0.721-8
30.0	1.293-7	1.275-7	1.231-7	1.159-7	1.115-7	9.819-8	9.066-8	6.669-8	5.215-8	1.088-8
40.0	1.578-7	1.556-7	1.506-7	1.427-7	1.378-7	1.219-7	1.127-7	8.312-8	6.510-8	1.345-8
50.0	1.792-7	1.768-7	1.715-7	1.633-7	1.580-7	1.403-7	1.299-7	9.601-8	7.531-8	1.587-8
60.0	1.961-7	1.937-7	1.883-7	1.799-7	1.742-7	1.552-7	1.438-7	1.065-7	8.372-8	1.773-8
70.0	2.106-7	2.080-7	2.024-7	1.937-7	1.878-7	1.676-7	1.554-7	1.154-7	9.054-8	1.934-8
80.0	2.228-7	2.201-7	2.142-7	2.054-7	1.993-7	1.782-7	1.654-7	1.230-7	9.697-8	2.074-8
90.0	2.332-7	2.303-7	2.244-7	2.154-7	2.092-7	1.874-7	1.740-7	1.297-7	1.023-7	2.198-8
100.0	2.421-7	2.393-7	2.333-7	2.243-7	2.179-7	1.955-7	1.817-7	1.356-7	1.071-7	2.310-8
200.0	2.933-7	2.902-7	2.840-7	2.748-7	2.681-7	2.427-7	2.265-7	1.714-7	1.369-7	3.068-8
300.0	3.132-7	3.100-7	3.038-7	2.949-7	2.882-7	2.625-7	2.456-7	1.880-7	1.516-7	3.514-8
400.0	3.207-7	3.175-7	3.114-7	3.029-7	2.965-7	2.712-7	2.544-7	1.965-7	1.598-7	3.815-8
500.0	3.219-7	3.189-7	3.131-7	3.050-7	2.989-7	2.744-7	2.579-7	2.008-7	1.644-7	4.030-8
600.0	3.199-7	3.171-7	3.116-7	3.040-7	2.981-7	2.745-7	2.585-7	2.026-7	1.668-7	4.190-8
700.0	3.167-7	3.140-7	3.086-7	3.012-7	2.957-7	2.729-7	2.574-7	2.030-7	1.680-7	4.311-8
800.0	3.125-7	3.098-7	3.046-7	2.975-7	2.922-7	2.703-7	2.552-7	2.023-7	1.683-7	4.406-8
900.0	3.077-7	3.051-7	3.001-7	2.933-7	2.882-7	2.670-7	2.525-7	2.011-7	1.679-7	4.479-8
1000.0	3.027-7	3.002-7	2.953-7	2.888-7	2.839-7	2.635-7	2.494-7	1.995-7	1.672-7	4.537-8

plasma in $eV.cm^{3}.s^{-1}$. Comparison with the results of Ref. [42] shows that

in the low-temperature region (for which we have only the results of

Ref. [42]) the agreement is sufficiently satisfactory. It should be noted

that in our calculations the effective recombination rate increases more

strongly with density. In the $T_e > 6$ eV region, where dielectronic

recombination makes an important contribution, the results of the present work

cannot be compared with those of Ref. [42] since the latter study was confined

to the consideration of the $T_e < 6$ eV region by not taking dielectronic

recombination into account. The results of calculation of the collisional

dielectronic recombination coefficient for the reaction $e + He^{+}$ show fair

agreement with the result given in Ref. [3]. Our values of the effective

ionization rate for the helium atom are also characterized by a stronger

increase with rise in density in comparison with the results of Ref. [42].

For the convenience of using the results we give: in Fig. 27 the

dependence of the effective ionization rate in a hydrogen plasma S_i on T_e (for

different n_e), in Fig. 28 the dependence of S_i on n_e (for different T_e),

in Fig. 29 the dependence of effective recombination rate α_{rec} on T_e (for
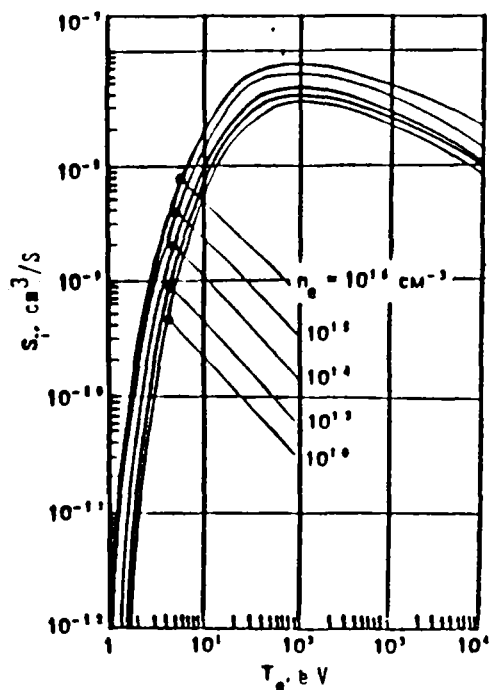
Fig. 27. Dependence of the effective
ionization rate in the hydrogen
plasma on T_e.
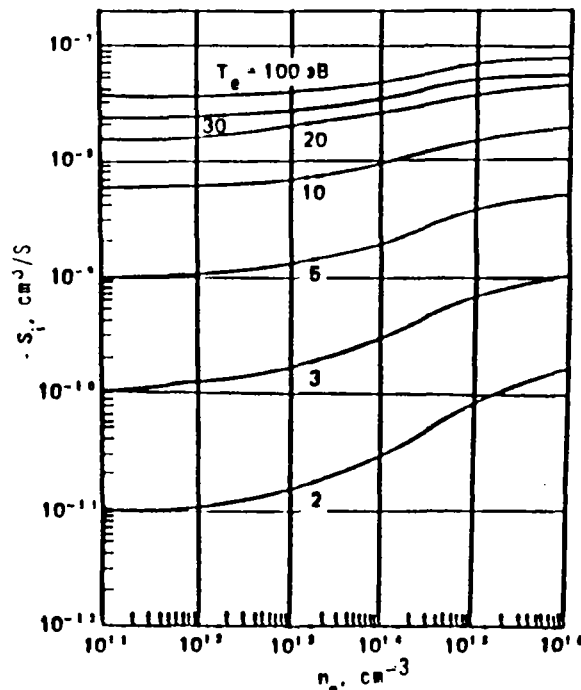
Fig. 28. Dependence of the effective
ionization rate in the hydrogen plasma
on n_e.

45
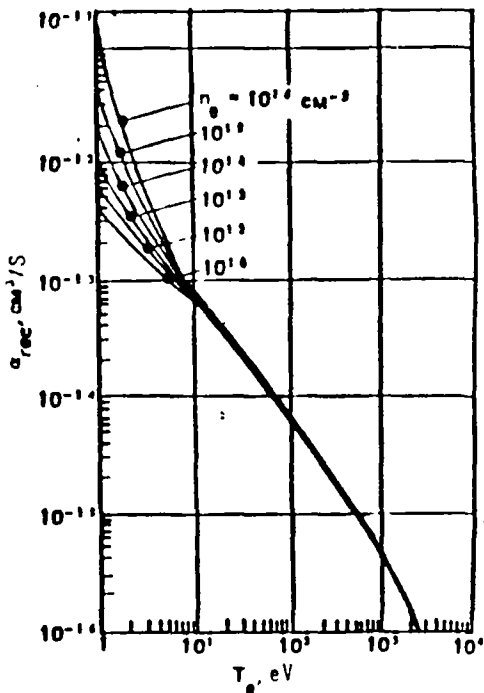
Fig. 29. Dependence of the
effective recombination rate in
the hydrogen plasma on T_e.
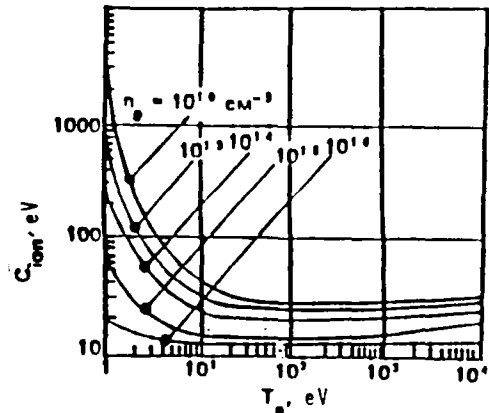
Fig. 30. Dependence of C_{ion}
in the hydrogen plasma on T_e.

different n_e) for a hydrogen plasma, in Fig. 30 the dependence of C_{ion} on T_e

(for different n_e), in Fig. 31 the dependence of the total reduced radiation

intensity of the hydrogen plasma on T_e, in Fig. 32 the reduced intensity of the

H_α-line and in Fig. 33 the reduced intensity of the H_β-line (we recall

that in order to obtain the true intensity, we have to multiply the reduced

intensity by $N_o n_e$, where N_o is the density of hydrogen atoms). Similar

results are presented for the helium plasma: in Fig. 34 the dependence of the

effective ionization rate on T_e (for different n_e) for helium, in Fig. 35 the

dependence of S_i on n_e (for different T_e), in Fig. 36 the dependence of the

effective recombination rate in the helium plasma on T_e (for different n_e), in

Fig. 37 the dependence of α_{rec} on n_e (for different T_e), in Fig. 38 the

dependence of C_{ion} (with He^+ ion formation) in the helium plasma on T_e and

in Fig. 39 the dependence of the reduced radiation power of the helium plasma on

T_e (for different n_e).

46
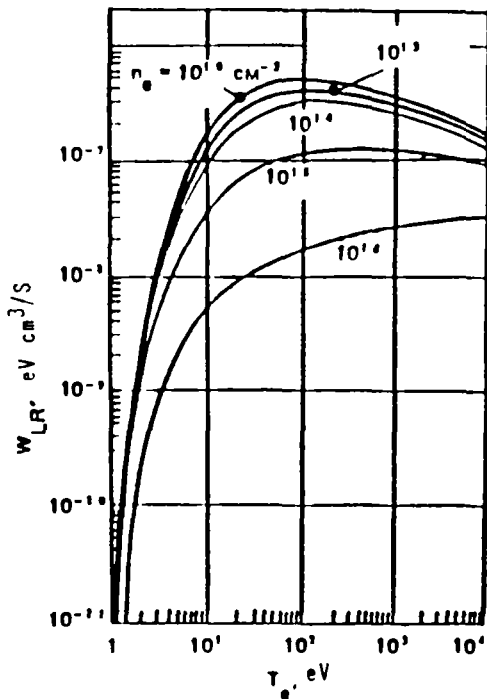
Fig. 31. Dependence of the reduced power of radiation of the hydrogen plasma on T_e.
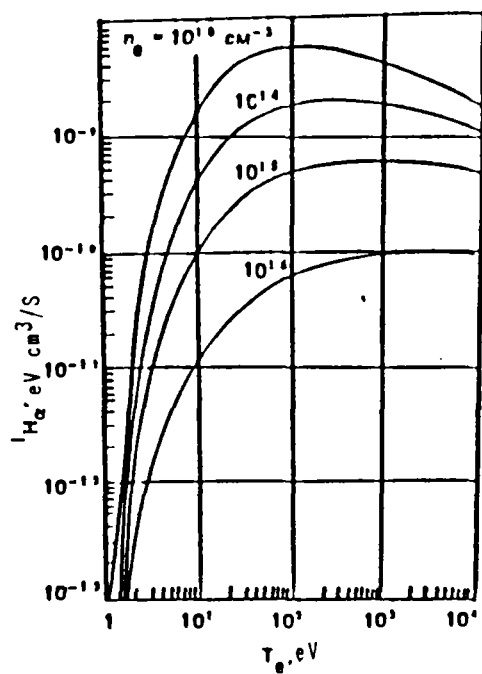
Fig. 32. Dependence of the reduced power of H_α line radiation on T_e.
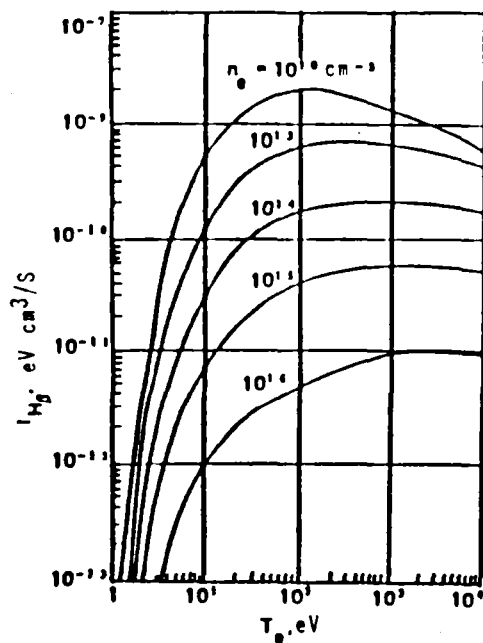
Fig. 33. Dependence of the reduced power of H_β line radiation on T_e.
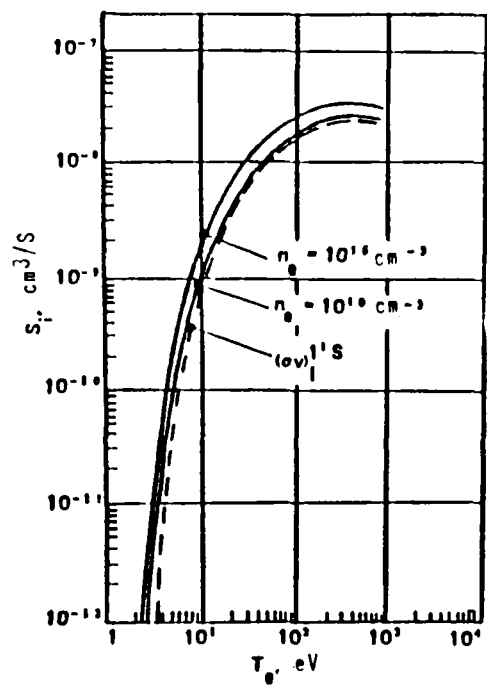
Fig. 34. Dependence of the effective ionization rate in the helium plasma on T_e.
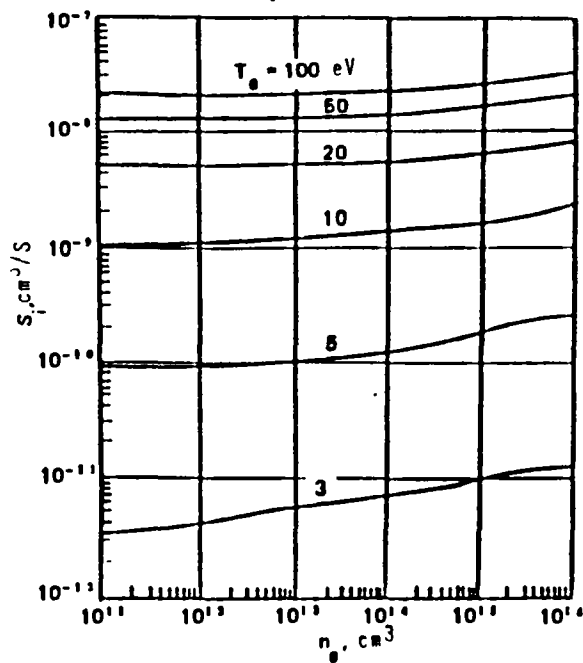
Fig. 35. Dependence of the effective ionization rate in the helium plasma on n_e.
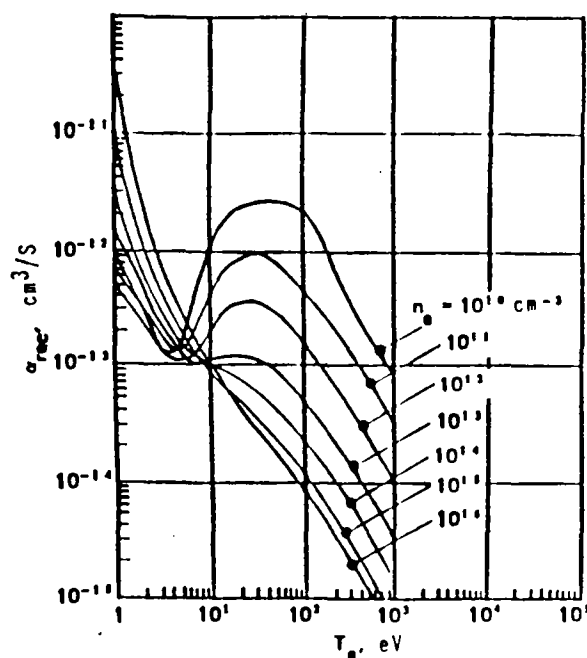
Fig. 36. Dependence of the effective recombination rate in the helium plasma on T_e.
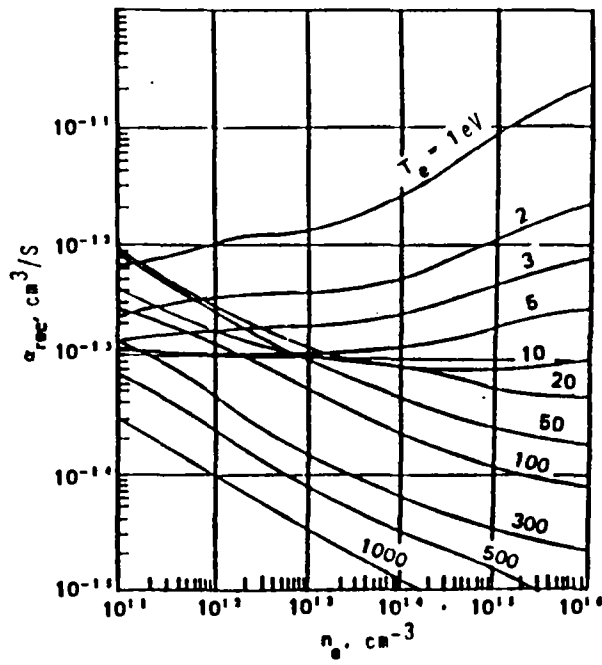
Fig. 37. Dependence of the effective recombination rate in the helium plasma on n_e.
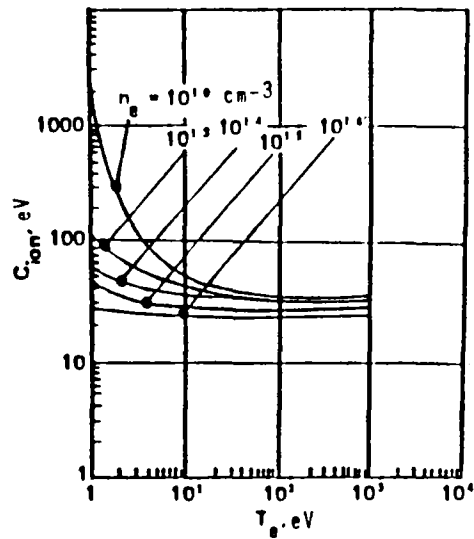
Fig. 38. Dependence of C_{ion} in the helium plasma on T_e.

48
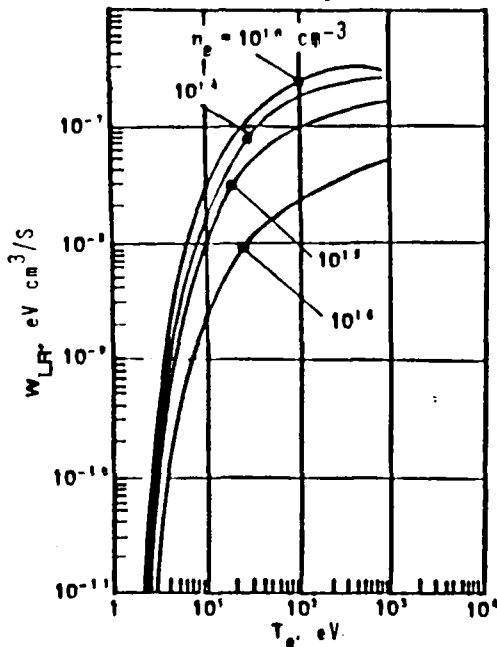
Fig. 39. Dependence of the reduced power
of radiation in the helium plasma on T_e.

In order to determine the effective rates of ionization and

recombination during the interaction of electrons with the He^+ ion, we can

recommend the results of a number of calculations for hydrogen-like ions with

$Z > 1$ (see, for example, Refs [2-4]), which agree satisfactorily with each

other in the region of interest to us.

REFERENCES

[1]   FUJIMOTO, T., IPPJ-AM-8, 1978.

[2]   BATES, D.R., KINGSTON, A.E., McWHIRTER, R., - Proc. Royal. Soc. Ser. A.
       - London, 1962, Vol. 267, p. 297.

[3]   BARNETT, C., HARRISON, M.F.A., (Eds) Applied Atomic Collision Physics.

[4]   GRIEM, H., Plasma Spectroscopy, Atomizdat (1967).

[5]   WIESE, W.L., SMITH M.W., GLENNON, B.M., Atomic transition
       probabilities. Vol. 1 - Washington: NBS, 1966.

[6]   JOHNSON, L.C., - Ap. Journal, 1972, Vol. 174, p. 227.

[7]   VAINSHTEIN, L.A., SHEVEL'KO, V.P., The Structure and Characteristics of
       Ions in a Hot Plasma, Nauka, Moscow (1986) (in Russian).

[8]   WESTERVELD, W.B., et al., - J. Phys. B, 1979, Vol. 12, p. 115.

[9]   GOSTEV, V.A., et al., Opt. Spektrosk. 48 (1980) 457.

[10]   VAN ZYL B., DUNN, G.H., et al., - Phys. Rev. A, 1980, Vol. 22, p. 1916.

[11]   FON, W.C., BERRINGTON, K.A., KINGSTON, A.E., - J. Phys. B, 1980,
        Vol. 13, p. 2309.

[12]   FON, W.C., BERRINGTON, K.A., BURKE, P.G., KINGSTON, A.E., - J. Phys. B,
        1981, Vol. 14, p. 2921.

[13]   BALUJA, K.L., McDOWELL, M.R.C., - J. Phys., 1979, Vol. B12, p. 835.

[14]   WILLIS, S.L., McDOWELL, M.R.C., - J. Phys., 1981, Vol. B14, p. L453.

[15]   FLANNER, M.A., MORRISON, W.F., RICHMOND, S.L., - J. Appl. Phys., 1975,
        Vol. 46, p. 1186.

[16]   OCHKUR, V.I., Zh. Ehksp. Teor. Fiz. 18 (1964) 1383.

[17]   BADNELL, N.R., - J. Phys., 1984, Vol. B17, p. 4013.

[18]   JANEV, R.K., LANGER, W.D., EVANS, K.E., Jr., POST, D.E., "Elementary
        Processes in Hydrogen-Helium Plasmas" (Springer-Verlag,
        Berlin-Heidelberg, 1987).

[19]   BERRINGTON, K.A., et al., - J. Phys., 1985, Vol. B18, p. 4135.

[20]   Atomic Data Workshop, Darsbury 1985, Warrington Laboratory, 1986.

[21]   MAZING, M.A., SLEMZIN, V.A., SHEVEL'KO, A.P., in: Atomic Collision
        Physics and Plasma Spectroscopy. Proceedings of the Physics Institute
        of the USSR Academy of Sciences No. 119 (1980) 169 (in Russian).

[22]   VAINSHTEIN, L.A., SOBELMAN, I.I., YUKOV, E.A., Excitation of Atoms and
        Broadening of Spectral Lines, Nauka, Moscow (1979) (in Russian).

[23]   OCHKUR, V.I., Zh. Ehksp. Teor. Fiz. 45 (1963) 734.

[24]   VAN REGEMORTER, H., - Ap. Journal, 1962, Vol. 132, p. 906.

[25]   BRANSDEN, B.H., DEWANGEN, D.P., - J. Phys., 1978, Vol. B11, p. 3425.

[26]   SINGH, C.S., SRIVASTAVA, R., RAI, D.K., - Phys. Rev. A, 1983, Vol. 27,
        p. 302.

[27]   SCOTT, T., McDOWELL, M.R.C., - J. Phys., 1975, Vol. B8, p. 1851.

[28]   FON, W.C., BERRINGTON, K.A., BURKE, P.G., KINGSTON, A.E., - J. Phys.,
        1979, Vol. B12, p. 1861.

[29]   JOHNSTON, A.R., BURROW, P.D., - J. Phys., 1983, Vol. B16, p. 613.

[30]   AMUS'YA, M.Ya., CHERNYSHEVA, L.V., SHEINERMAN, S.A., Zh. Tekh. Fiz. 54
        (1984) 1454.

[31]   TULLY, J.A., - J. Phys. 1980, Vol. B13, p. 4845.

[32]   BURRELL, C.F., KUNZE, H.J., - Phys. Rev. A, 1975, Vol. 18, p. 2081.

[33]   KHAYTALLAH, G.A., CHEN, S.T., RUMBLE, J.K., Jr., - Phys. Rev. A, 1978, Vol. 17, p. 513.

[34]   MOISELWITSCH, B.L., SMITH S.J. - Rev. Mod. Phys., 1968, Vol. 40, p. 335.

[35]   BRANSDEN, B.H., WINTERS, K.H., - J. Phys., 1975, Vol. B8, p. 1236.

[36]   BELL, K.L., GILBODY, H.B., HUGHES, J.G., KINGSTON, A.E., SMITH, F.L., - CLM-R216, 1986.

[37]   ZHDANOV, V.P., Fiz. Plazmy 5 (1979) 572.

[38]   VAINSHTEIN, L.A., SOBELMAN, I.I., YUKOV, E.A., Excitation of Atoms and Ions by Electrons, Nauka, Moscow (1973).

[39]   VRIENS, L., SMEETH, A.H.M., - Phys. Rev. A, 1980, Vol. 22, p. 940.

[40]   DRAWIN, H.W., EMARD, E., - Physica 85 c, 1977, p. 333.

[41]   JOHNSON, L.C., HINNOV, E., - JQSRT, 1973, Vol, 13, p. 333.

[42]   DRAWIN, H.W., EMARD, F., - Z. Physik, 1971, Vol. 243, No. 5, p. 326.